Acoustoelectronic instability in piezosemiconductors

V. M. Rysakov

(Submitted 30 May 1990; resubmitted after revision 26 July 1991)
Usp. Fiz. Nauk **161**, 1–37 (December 1991)

Studies of the development of acoustoelectronic instability in AIIIBV and AIIBVI bulk piezosemiconductors are reviewed. The results of the classical theory of linear and nonlinear acoustoelectronic interactions are briefly summarized and the energy approach to this problem is discussed. An analysis is then given of the properties of instabilities and of instability development, including coherence effects. Experimental methods are briefly surveyed with particular reference to the fundamentals of the most effective method, namely, Mandel'shtam–Brillouin scattering. The results of the most significant experiments are presented, and an attempt is made to interpret them in terms of a unified model. It is emphasized that the high gain regime, in which a propagating acoustoelectronic domain is produced, requires further investigation.

INTRODUCTION

In 1961, Hutson, McFee, and White[1] discovered that acoustic signals were amplified by piezosemiconductors when an electric field was applied to them. The amplification was so large that it gave rise to acoustic instability, with the thermal acoustic noise rising to a very high level. The phenomenon immediately attracted considerable attention. For about 15 years there was a veritable flood of papers on this subject, followed by something of a decline, despite the fact that many of the fundamentals of the effect were not understood. The total number of publications in this field now stands at over a thousand. Since many of the results have already been examined in existing reviews,[2-7] we shall concentrate our attention on the more recent publications. We note that our bibliography does not claim to be exhaustive, and we offer our apologies in advance to authors whose work has not been included in this review.

The acoustoelectronic interaction is of considerable interest from many points of view. In particular, the process involves different linear, nonlinear, and parametric interactions, self-organization occurs of a quasidense quasimonochromatic flux out of thermal noise, and so on. Moreover, the parameters of the acoustoelectronic interaction can be varied quite readily between wide limits by varying the external conditions, so that the phenomenon can be used for modeling purposes in many cases.

Possible technological applications of the effect are also of interest. In particular, it can be used as a basis for an electric-signal amplifier for the decimeter wavelength range, offering unique properties, e.g., high gain (tens of dB), relative passband of the order of 1/3, the possibility of electronic tuning, and the absence of external circuitry. After the first few years of investigation, it was found that there was no fundamental bar to the development of such an amplifier,[8] but it also became clear that the amplifier would not work in practice, principally because of the anomalously high amplification of noise. The situation was not clarified despite numerous experimental and theoretical publications. Indeed, a peculiar conceptual *cul de sac* was encountered, and there was a general loss of interest in the subject.

Nevertheless, since the problem remained unsolved either from the fundamental or technological points of view, some research work has continued and new ideas were recently expressed on the details of the processes that accompany the acoustoelectronic interaction. These ideas are incorporated in our review which is confined to acoustoelectronic interactions in AIIBVI and AIIIBV piezosemiconductors in bulk.

1. THEORY OF THE ACOUSTOELECTRONIC INTERACTIONS

1.1. Simplified physical picture of the process

It is well known that the deformation of a piezoelectric material can produce an electric field in the direction of deformation.[3] Correspondingly, elastic waves propagating in a piezoelectric medium give rise to a longitudinal electric field whose spatial period is equal to that of the elastic waves.

If the crystal is a semiconductor, the distribution of its free electrons is modulated in space by the piezoelectric field of the elastic wave with the same spatial period. Free electrons tend to screen the field produced by the wave, but the finite Debye screening length and the finite Maxwell relaxation time constant ensure that this screening is not complete. The residual piezoelectric field induces an electron-density wave that propagates with the velocity of sound; i.e., the field produces an acoustoelectric current. In a crystal of finite resistivity, this current is maintained by the energy drawn from the acoustic wave. This gives rise to an electronic attenuation coefficient α_e which is added to the usual lattice attenuation coefficient α_L. The application of an external electric field that produces an electron drift at the velocity of sound should then reduce the electronic attenuation to zero and, when the electron velocity is high enough, it should give rise to amplification. In principle, the amplification process is analogous to the amplification of electromagnetic waves in a TWT.

1.2. Linear theory of the acoustoelectronic interaction

This theory was developed as far back as 1962 by Hutson and White[9-11] and, independently, by Gurevich.[12-14] It has frequently been presented in a variety of publications. We shall therefore confine ourselves to a very brief account of it.

 0038-5670/91/121027-20$01.00

We shall assume that the piezosemiconductor occupies the entire half-space to the right of the $z = 0$ plane and that the z axis lies along one of the symmetry axes of the crystal. A plane monochromatic acoustic wave is excited on the surface of the medium and is characterized by deformation $S = S_0\exp[i(qz - \Omega t)]$ where q is the wave vector and Ω the frequency. We thus have a one-dimensional problem in which an infinite plane wave that depends only on the coordinate z propagates in the sample. This is one of the basic assumptions that restrict the range of amplification of this particular special solution.

A simple model of an n-type extrinsic semiconductor is used. It is assumed that the electron distribution is nondegenerate and is described by the Maxwell–Boltzmann statistics. The wavelengths are such that the hydrodynamic approximation is valid ($ql < 1$) and the electrons have an isotropic reduced mass m^*. It is also assumed that an external source produces a constant electric field E_0 in the sample. Finally, the situation is described by the equation of state of the piezoelectric medium, the wave equation, the Poisson equation, the continuity equation, and the current equation.

This set of equations is solved by the method of slowly-varying amplitudes. It is clear that, because of nonlinearity, the propagation of a wave in the sample may be accompanied by the generation of harmonics, and the elastic and electron-density waves may not be sinusoidal. The determination of their waveform constitutes the so-called fast problem.[15,16] On the other hand, the variation of the wave amplitude with distance for a constant waveform is the concern of the so-called slow problem. It is clear that if the incident wave is sinusoidal and its amplitude is small (the relevant criterion will be reproduced later), the elastic and electron-density waves can be expanded into a Fourier series, and terms of order higher than the first discarded; i.e., we can assume that the waves are purely sinusoidal. Accordingly, we seek the complex wave amplitudes in the form

$$\begin{aligned} S &= S_1(z)\exp[i(qz - \Omega t)], \\ n &= n_1(z)\exp[i(qz - \Omega t)] + n_0, \\ E &= E_1(z)\exp[i(qz - \Omega t)]. \end{aligned} \tag{1}$$

This transforms the differential equations into a set of algebraic equations for the amplitudes. By combining these equations, we obtain what is essentially a dispersion relation.

The problem can be solved in two ways. In the first method, used in the majority of publications (see the reviews in Refs. 3 and 4), we eliminate the electric wave and find the dispersion relation for the mechanical part of the coupled wave, which is then used to determine the modified modulus of elasticity c'. In the second method, due to Pustovoĭt,[6] the mechanical part of the wave is eliminated and a solution is sought for the electric part, i.e., for the modified permittivity ε'. In principle, the two methods are equivalent.

The solution of the problem leads to the following expressions for the velocity of sound and the attenuation of sound, respectively:

$$\begin{aligned} v_S &= v_0\left\{1 + \varkappa^2\frac{\beta_E^2 + [(1 + x^2)/4]}{\beta_E^2 + [(x + x^{-1})^2/4]}\right\}, \\ g &= g_M\frac{2\beta_E}{\beta_E^2 + [(x + x^{-1})^2/4]}, \end{aligned} \tag{2}$$

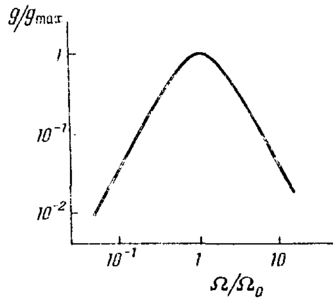

FIG. 1. Relative gain as a function of relative detuning.

where v_0 and v are the velocities of sound in the piezoelectric medium and the piezosemiconductor, respectively, $\gamma = 1 - (\mu E_0/v)$ is the supercriticality, $\gamma_0 = 2(\Omega_e/\Omega_D)^{1/2}$ is the optimum supercriticality, $\beta_E = \gamma/\gamma_0$ is the normalized supercriticality, $\Omega_0 = (\Omega_c\Omega_D)^{1/2}$ is the frequency at maximum gain, $\Omega_c = \sigma/\varepsilon$, $\Omega_D = v^2/D_e$, $x = \Omega/\Omega_0$ is the relative detuning, $\sigma = n_0 e\mu$ is the conductivity, $g_M = \varkappa^2\Omega_0/8v$ is the absolute maximum gain, $\varkappa$ is the electromechanical coupling coefficient, $D_e = k_B T/e$ is the diffusion coefficient, $\alpha_e = 2g$ is the power and amplitude gain, μ is the mobility, e is the electron charge, k_B is the Boltzmann constant, and T is the temperature.

The amplitude of the piezoelectric field of the wave in the semiconductor $E_1 = E_{10}f_1$ is related to the amplitude of the elastic wave by $E_{10} = dS_1/\varepsilon$, where the screening factor is given by

$$f_1 = \frac{\beta_E + (ix/2)}{\beta_E + [i(x + x^{-1})/2]}. \tag{3}$$

Accordingly, the amplitude of the self-consistent electron-density wave is $n_1 = \mu E_1 n_0 f_2/v$ where $f_2 = \{\gamma_0[\beta_E + (ix/2)]\}^{-1}$.

We must now analyze the above expressions. First, it is obvious that the influence of the electrons exhibits a resonance; i.e., a maximum occurs at frequency Ω_0 (Fig. 1) for which the wave vector is equal to the reciprocal of the Debye length. At higher frequencies, the spatial modulation depth of the electron distribution is reduced, and this leads to a reduction in the strength of the interaction. On the contrary, at lower frequencies, the electron distribution can follow even the screened field, so that the electrons are not dragged by the piezoelectric field of the wave; i.e., the acoustic current tends to zero. The contribution of electrons to wave attenuation (amplification) also tends to zero.

Next, the sign of the interaction depends on the sign of the supercriticality β_E, i.e., on the ratio of the electron drift velocity to the velocity of sound (Fig. 2), which depends on

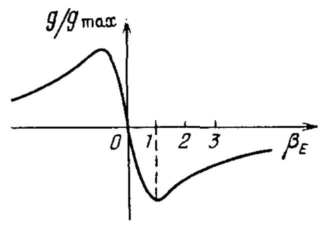

FIG. 2. Relative gain as a function of normalized supercriticality.

TABLE I. Frequency at maximum gain F_0, optimal supercriticality γ_0, and maximum gain g_M as functions of concentration for the T2 wave in standard CdS samples with mobility 250 cm^2 V^{-1} s^{-1}.

n_0, cm^{-3}	Ω_c, s^{-1}	Ω_D, s^{-1}	F_0, GHz	γ_0	g_M, dB/cm
10^{14}	$5\cdot10^9$	$4{,}9\cdot10^9$	0,79	2	$1{,}1\cdot10^3$
10^{15}	$5\cdot10^{10}$	$4{,}9\cdot10^9$	2,5	6,6	$3{,}5\cdot10^3$
10^{16}	$5\cdot10^{11}$	$4{,}9\cdot10^9$	7,9	20	$11\cdot10^3$

the phase of the electron wave relative to the piezopotential wave.

The gain depends on the supercriticality. At first, the amplification of the field leads to a rise in the gain, and then the gain reaches its maximum for optimum supercriticality $\beta_E = 1$. Further increase in the field is accompanied by a reduction in gain. A similar dependence is produced when the phase of the electron-density wave shifts relative to that of the electric-field wave. As an example, Table I lists the optimum supercriticalities and the numerical values of the gain in CdS for typical electron concentrations. We note that the gain is very high and does not vary to any great extent on the left-hand (downward) branch of the curve as the concentration is increased and the gain curve shifts upward and to the right.

We emphasize that the frequency dependence of the transmission factor of this acoustic amplifier depends on the frequency dependence of the gain, but differs from the latter because it appears in the argument of the exponential as a cofactor of the path length. The passband is infinite near the entrance plane of the sample, but decreases in the course of propagation (Fig. 3). For limiting values, determined by the linear dynamic range (10^6–10^8), this is a relatively weak dependence and the relative passband in this range is $\Delta\Omega/\Omega_0 \sim 1/3$.

It is important to note that the total gain is determined by the difference between electron (α_e) and lattice (α_L) attenuation coefficients. Accordingly, the frequency dependence of the total gain is also found to depend on this difference. Obviously, lattice attenuation can be neglected when $\alpha_e \gg \alpha_L$, and all the foregoing discussion is then valid. However, when the electron gain is comparable with the lattice attenuation, the frequency dependence of both terms has to be taken into account. We know that the frequency dependence of the lattice attenuation is $\alpha_L \sim \Omega^p$ where p ranges from 2 (high temperatures, Akheizer attenuation mechanism) to 1 (low temperatures, Landau–Rumer attenuation mechanism).[18] It is shown in Ref. 19, that when α_e and α_L are comparable, the frequency at maximum gain shifts downwards and is given by $\Omega_{max} = \Omega_0(2-p)/(2+p)$, which must be taken into account in the interpretation of experimental data.

There is an analogous filtration of the angular spectrum (Fig. 3), due to the angular dependence of the gain. For the same limiting values of the gain, the width of the angular spectrum is of the order of 5–10°. It will be clear later that knowledge of this quantity is essential in the analysis of the amplification of noise.

As mentioned above, free electrons are also found to affect the velocity of the acoustic wave [see (2)]. It is clear that this is significant only near the frequency corresponding to maximum gain and zero supercriticality for which the gain reaches a few percent. Physically, this is due to the screening of the piezoelectric field by free electrons, which leads to a reduction in the effective stiffness. For commonly used supercriticalities, we have $\gamma > 1$ and it may be considered that acoustic waves do not in most cases exhibit dispersion under such conditions.

1.3. Nonlinear theory

It is obvious that the amplification of a propagating acoustic wave in a crystal is eventually limited by nonlinear mechanisms that prevent an infinite rise in the signal amplitude. Estimates show that the inelastic nonlinearity is usually negligible in this process. The most important effect is associated with the electron nonlinearity which becomes significant at much lower acoustic flux densities. Physically, this nonlinearity is due to the remodulation of the electron current.[20] When the modulation amplitude n_1 is comparable with n_0, any further increase in the wave amplitude leads to a distortion of electron-density modulation waveform (Fig. 4). When the wave amplitude is large enough, all the free electrons are confined to a single half-wave, so that there are practically no electrons in the other half-wave.

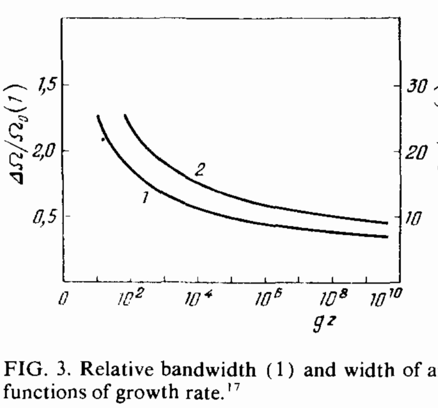

FIG. 3. Relative bandwidth (1) and width of angular spectrum (2) as functions of growth rate.[17]

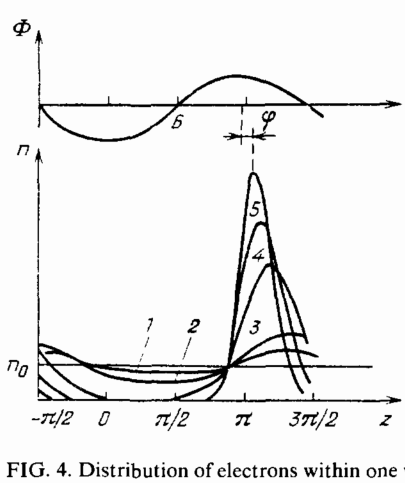

FIG. 4. Distribution of electrons within one wave for $e\Phi/k_B T = 0.1(1)$, 2.0(2), 5.0(3), 7.0(4), 10(5) and the distribution of potential within one wave (6).[20]

It is clear from Fig. 4 that 100% modulation of the electron flux occurs for $e\Phi \sim 2k_B T$ (for $\beta_E \ll 1$). However, since the nonlinearity becomes significant much earlier, it is common to use $e\Phi_1/k_B T$ as the nonlinearity parameter. The nonlinearity is weak for $e\Phi_1/k_B T < 0.1$, intermediate between 0.1 and 2–4, and strong above 4. In the last case, the thermal energy of electrons is insufficient to overcome the potential barrier Φ_1 produced by the piezoelectric field; i.e., the electrons are all trapped in the potential wells and travel with the velocity of sound.

A closed solution of the problem can be constructed only for weak nonlinearity and deep saturation. A number of different methods is available for this. In the case of a weak nonlinearity, the electron density is expanded into a series and the second term is retained as a small correction[21,22] that leads to a reduction in gain. For a strong nonlinearity, the exponential rise in the size of the signal slows down and the increase becomes sublinear. This is formally described as a reduction in gain. When lattice attenuation is taken into account, the signal reaches the saturation level given by the expression[20]

$$I_{a,sat} = envE_0/\alpha_L \tag{4}$$

The intermediate nonlinearity is the most difficult to analyze. It requires the inclusion of a large number of terms in the expansion,[20,23,24] which in turn involves a numerical calculation. However, there is also another approach proposed by Gulyaev[15,16] who constructed the solution in the form of functionals for arbitrary nonlinearity. For large and small nonlinearities, the functionals can be simplified and the solution assumes the usual form. Interpolation formulas are used for the intermediate nonlinearity. However, these formulas are relatively complicated and are difficult to use in the analysis of the processes taking place.

Tien's solution[20] is the clearest and relies on a computer to plot out a large number of graphs characterizing this process. The solution employs a Fourier expansion and the examination of the self-consistent problem with the retention of a sufficient number of harmonics. The first step is to consider the fast problem and to determine the form of the electron distribution for a monochromatic elastic wave of arbitrary amplitude in an arbitrary drift field (see Fig. 4). It is clear that an increase in the amplitude of the modulating wave is accompanied by a conversion of the sinusoidal waveform into short Gaussian pulses that become narrower and shift toward the piezopotential minimum as the amplitude increases.

Next, the current flowing through the sample is calculated for a constant amplitude of the acoustic wave (Fig. 5). As expected, at low intensities, the ohmic current, $j_0 = \mu e n_0 E_0$, flows through the sample, but the current is significantly reduced when the intermediate nonlinearity is reached. The current reaches the saturation level $J_s = en_0 v$ in the case of the strong nonlinearity. This corresponds to the complete trapping of electrons by the piezopotential wells and to their motion with the velocity of sound independently of the strength of the drift field.

Calculations of the gain (Fig. 6) for this situation show that the fall in the current from its ohmic value is accompanied by a fall in gain, and the linear dynamic range expands with increasing drag field.

It is clear from the foregoing that the onset of appreciable nonlinearity ensures that the electron-density wave becomes nonsinusoidal; i.e., the modified waveform contains a large number of harmonics and the inverse piezoelectric effect gives rise to the excitation of the corresponding harmonics in the elastic wave. Since the contribution of dispersion is negligible, this forced excitation is in phase with the free wave. This should give rise to the efficient generation of harmonics.[16,20,25] However, in practice, the more commonly observed effect is the generation of subharmonics rather than harmonics. This will be discussed below.

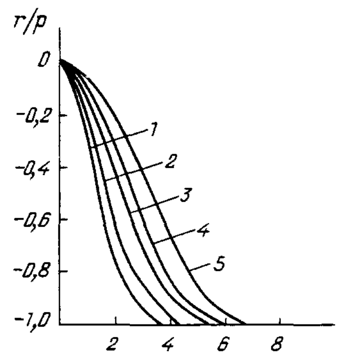

FIG. 5. Relative current saturation factor $r/p = [1 - (j_s/j)]/x\gamma_1$ as a function of the relative amplitude $e\Phi_1/k_B T$ for $\beta_E = 0.1(1)$, 0.5(2), 0.9(3), 1.1(4), 1.5(5) for $x = 1$ (Ref. 20).

1.4. Energy approach

It is clear from the foregoing presentation that the exact solution of the acoustoelectronic interaction problem for an arbitrary wave amplitude is possible only by numerical methods. On the other hand, an exact solution would not be particularly useful in practice because of the parasitic effect of the many factors that are ignored in the above idealized model, so that the final precision of such calculations is not high. It would therefore be desirable to have a method of solution that could, on the one hand, ensure satisfactory precision (5–10%) and, on the other, allow simple analysis for any degree of nonlinearity.

These conditions seem to be satisfied by the energy approach to the interaction between acoustic and electron waves. The elements of this approach were first introduced by Weinrich[26] who calculated the acoustoelectric current in the linear regime. He showed that, in the linear case, the

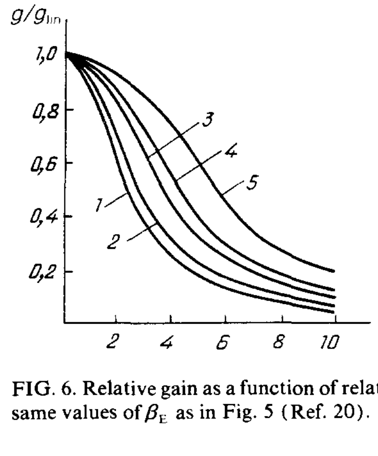

FIG. 6. Relative gain as a function of relative amplitude $e\Phi_1/k_B T$ for the same values of β_E as in Fig. 5 (Ref. 20).

acoustoelectric current is given by the following expression: $j_{ae} = -2\alpha_L \mu I_a / v$. The basic validity of the energy approach, at least in principle, was then demonstrated by Pomerantz[27] who did not, however, report a complete solution.

The complete implementation of the method was reported for the first time in Refs. 28 and 29. It is clear from the above discussion that an acoustic wave has a mixed electromechanical character in a piezoelectric medium, and that the ratio of the current densities associated with the waves, I_M/I_e, is determined by the electromechanical coupling factor $\varkappa$: $I_e = \varkappa^2 I_M$. The energy of interaction between the electron wave and the electric field of the acoustic wave is expended in increasing the total energy. It is easy to show that the change in the energy produces a change in the amplitude by the amount

$$dE_{10} = \varkappa^2 \Delta n_{\text{eff}} \sin\varphi \cdot dz/\varepsilon, \tag{5}$$

where $\Delta n_{\text{eff}} = Q\Delta n$, $\Delta n = N_{\max} - N_{\max}$, Q is a coefficient representing the particular form of the distribution, and $N_{\max}$ and $N_{\min}$ are, respectively, the number of electrons in the two half-waves (see Fig. 4). Direct calculation shows that Q varies from $\pi/4$ in the linear case to 1 in the case of a strong nonlinearity; i.e., the variation is relatively slight. We can therefore always assume that, to a good approximation, $Q = 1$.

The expression given by (5) is the basic equation for the change in the amplitude of the electric field, and, correspondingly, the amplitude of the deformation accompanying the interaction with the self-consistent electron-density wave. In the above terminology, this is the solution of the slow problem. However, since the energy approach is known to be insensitive to the fine details of the processes taking place, we need not have an exact solution of the fast problem: $Q \simeq 1$ for any waveform. This is confirmed by calculations made for linear and strongly nonlinear cases, when the results obtained by this method are found to agree with those already known.

It is clear from (5) that the variation in the wave amplitude is determined by the dependence of the effective number of electrons Δn_{eff} and their phase shift φ on the piezoelectric field amplitude. The wave amplitude varies exponentially in space if, and only if, the effective number of electrons is proportional to the piezoelectric field amplitude, but the phase does not depend on this amplitude. If, on the other hand, the effective number of electrons is constant and independent of the piezoelectric field amplitude, and the phase is constant, the wave amplitude varies linearly in space. However, since for a constant number of electrons, screening becomes weaker with increasing amplitude, which leads to a reduction in the phase shift, the real increase in amplitude is slower (for $\beta_E < 1$).

The energy approach to the solution of the problem of interaction between acoustic and electron waves is thus seen to lead in limiting cases to results that agree with those obtained by traditional methods. This confirms their validity. However, the energy method has significant advantages as compared with the traditional approach. First, it emphasizes the locality of the interaction: the increase in the amplitude of a particular wave period depends only on the behavior of the electron distribution at the given wavelength. This interaction is local both in the longitudinal coordinates, which follows from the procedure used to construct the solution, and in transverse coordinates, which follows from the principle underlying the calculation. The necessary condition for the validity of this method is that the variation with respect to the Riemann variable $t - (z/v)$ is slow; i.e., the method is valid even for very short pulses (one or two periods). Coherence in the transverse coordinate is necessary on the scale of a few wavelengths in order to ensure that the wave process can occur.[30] This extension of the validity of the model will be necessary later when we come to analyze the evolution of an acoustoelectric domain. Second, the method has the advantage that it provides us with a unified approach to states with any degree of nonlinearity, including intermediate nonlinearity. This is also important in the analysis of the evolution of a domain.

2. EVOLUTION OF ACOUSTIC INSTABILITY

We have already considered the amplification of a plane monochromatic wave generated on the boundary of a sample. When the acoustic instability is examined, it is important to allow for the fact that, first, the source of nucleating noise may be distributed uniformly throughout the sample (thermal noise) and, second, the nucleating noise has a wide temporal and spatial spectrum; i.e., the longitudinal and transverse multimode nature of the signal must be allowed for. In the linear regime, the individual modes do not interact, so that the generalization of the single-mode theory to this regime presents no particular difficulty. On the other hand, the nonlinear regime requires separate analysis.

2.1. Longitudinal distribution of current in the linear regime

We showed in the last section (see Fig. 3) that, in the case of high gain, for which the process is usually analyzed, the amplification bandwidths (temporal and spatial) undergo very little variation. We may therefore consider them to be constant for any growth rate, and refer them back to the cathode.

Let us now consider the transient regime (Fig. 7) in this approximation. The field is applied at $t = 0$ at which time the noise within the amplification bandwidth has a random profile in the form of a quasimonochromatic oscillation with mean wavelength equal to the reciprocal of the Debye length (which corresponds to the gain maximum). When the field

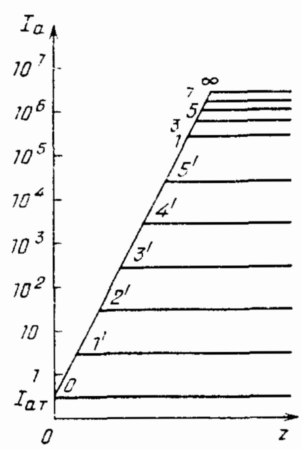

FIG. 7. Acoustic noise flux as a function of position along the specimen in the linear ($t = 0$–$5'$) and nonlinear ($t = 1$–∞) regions in the ideal case.

is applied, this profile begins to move to the right and its amplitude increases (convective instability[2]). The result is that the flux envelope in the sample takes the form of an exponential followed by a plateau. The plateau eventually shrinks and (at time $t = L/v$) disappears altogether; i.e., the distribution becomes a pure exponential.

It is shown in Refs. 17, 22, and 28 that the noise distribution is then described by the equation

$$dI_a/dz = (2g - \alpha_L)I_a + \alpha_L I_{aT} + 2g_0 I_{aT}, \quad (6)$$

where I_{aT} is the initial thermal-noise intensity within the amplification bandwidths and $g_0 = g|_{\gamma=1}$. The solution of the equation then takes the form

$$I_a = I_{aT}\{2[\exp(2g - \alpha_L)z - 1][(g_0 + g)/(2g + \alpha_L)] + 1\}. \quad (7)$$

Hence it is clear that for $2g \gg \alpha_L$, and as the acoustic instability develops, the solution has a different structure in the following two limiting cases. When $z < 1/2g$ (in the initial region) the first term can be neglected and the noise is practically the same as in the absence of amplification. In the other part of the sample, where $z > 1/2g$, we can neglect the second term. Hence, the flux structure in this region is such that intrinsic noise can be ignored. The flux in this region is wholly determined by amplified noise from the nucleating region. We therefore conclude the entire sample is naturally divided into the nucleating-signal generator and the ideal noiseless amplifier in which the "frozen" fluctuation from the nucleating-signal generator propagates with growing amplitude.

The output of the effective nucleating-signal generator is produced as a result of interference between a large number (up to 10^9) of modes and takes the form of a quasimonochromatic wave with mean frequency equal to the frequency at maximum gain and coherence length determined by the passband, i.e., of the order of three wavelengths. Phase fluctuations are equivalent to a frequency variation within the limits of the passband, whereas amplitude fluctuations are described by the Maxwell–Boltzmann distribution with modulation depth not exceeding 50% with a probability of 70%.

2.2. Transverse structure of the flux

We know[30] that the transverse structure of the noise flux in a passive medium is described by the van Cittert–Zernike theorem. The theorem is generalized in Ref. 31 to an active medium in which gain is a function of the transverse coordinate. However, its generalization to the case where the gain is a function of direction, as it is in the case of the acoustoelectronic interaction, has encountered certain difficulties.

It is more convenient in this case to use the spectral approach in which Kotel'nikov–Shannon trial functions[22,32,33] are used as the basis functions instead of the usual plane waves. This method has been used to show that the influence of the amplification process on transverse coherence is significant in this case if $g/q > \vartheta_0^2/(1 - \vartheta_0)^2$ where ϑ_0 is the angle for which the first nonzero term of the expansion of g into a power series in ϑ is found to vanish. It is readily seen that, in the case of the acoustoelectronic interaction, the weak dependence of gain on angle means that the above inequality is not met, so that amplification does not have a fundamental effect. For practical purposes, the coherence length is determined by the van Cittert–Zernike theorem. Even near the anode, the coherence length does not exceed a few dozen wavelengths, so that the flux should split into a set of coherent tubes. This shows that the plane-wave model used in theoretical analyses does not correspond to reality and one can hardly expect good agreement with experiment.

2.3. Effect of noise near the cathode

Experiments show that noise near the cathode (and not the thermal noise) is often the nucleus for developing noise flux. Noise near the cathode is due to two factors. First, it is associated with the flow of electric current through a contact, which is analogous in origin to electric contact noise. Second, it is due to the shock excitation of the cathode surface layer, which produces wave packets. It is precisely this that is largely responsible for the nucleation of a domain, and we shall therefore discuss it in greater detail.

Since the work functions of a semiconductor and a metal are necessarily not very different even in the case of an 'ohmic' contact, and since the surface layer is damaged during crystal processing, there is a transition layer between the bulk crystal and the metal. This layer constitutes an acoustic resonator that is excited by the leading edge of the incident drift-field pulse, and continues to emit acoustic radiation at its natural frequency for a certain period of time. If the surface is not damaged, the layer thickness is of the order of the Debye length, and its natural frequency is close to the frequency at maximum gain. Since fluctuations in electron concentration are significant in a layer of this thickness, the natural frequency of the layer may fluctuate from pulse to pulse. On the other hand, the natural frequency is lower when the surface is damaged, and this is indeed observed experimentally.[34]

Since the leading edge of the field pulse is usually long in comparison with the period of the oscillations, the shape of the emitted packet is different from the shock shape, and is determined by the convolution of the spectral density of the pulse and the transmissivity of the layer. The packet is expected to have a smooth bell-shaped envelope whose length is somewhat greater than the length of the leading edge of the pulse, and whose amplitude is just above the thermal level.[34] Attempts to estimate this amplitude by expanding the pulse sequence into a discrete Fourier series[35] cannot be regarded as valid because the pulse repetition period is long in comparison with the length of the packet.

The properties of this nucleating noise are different from those of equilibrium thermal noise. First, it is emitted by a localized source. Second, its temporal and, consequently, longitudinal coherence is significantly greater, i.e., of the order of the leading edge of the field pulse. Third, its transverse coherence is much greater because it is determined by the inhomogeneity of the layer on the contact surface. There are as yet no experimental data on this field, but physical considerations suggest that modern technologies available for the deposition of contacts can produce areas of constant thickness over linear dimensions of the order of 10–1000 μm. Another significant point is that, from the cathode onward, the amplitude flux splits into a set of parallel coherence tubes whose radius remains practically constant along the entire length of the sample.

The properties of this nucleating noise must be taken into account in the interpretation of experimental data together with the equilibrium thermal noise, since the two intensities are comparable.

2.4. Effect of nonlinearity on the evolution of flux coherence

The effect of nonlinearity on transverse structure has not been examined at all (it is meaningless on the one-dimensional model), whereas its effect on longitudinal structure is discussed in Ref. 36 in which it is shown that, in general, the coherence length can rise or fall depending on the signs of the coefficients in the solution. Since these signs have not been determined theoretically or experimentally, it is hardly possible to perform a comparison with experiment. Moreover, the solution is valid only for weak nonlinearity, and this restricts its range of validity.

3. EXPERIMENTAL METHODS FOR THE INVESTIGATION OF ACOUSTOELECTRONIC INSTABILITY

3.1. Electrical and acoustic methods

Historically, the first method was based on a study of the current-voltage characteristic.[37] It was found that the current-voltage characteristic had a "knee" at the threshold field, at which the linear portion turned over into a practically horizontal plateau. For a pulsed field, the current pulse had the following characteristic shape: The current was initially constant and equal to its ohmic value, but then (at low gain) it began to fall in step-like manner (with a period $T = L/v$), tending to a saturation level; at high gain, the current began to oscillate between the ohmic value and the saturation level with the period $T = 2L/v$ (Ref. 38). It is precisely these oscillations that were used to establish for the first time the domain character of the developing instability. However, it is now common to sue the single-transit regime in which the oscillations cannot be seen.

The length of the ohmic plateau (the so-called incubation time), is a measure of the time necessary for the development of the acoustic flux from the initial value I_{aT} to the onset of the intermediate nonlinearity I_{an} (when about 10% of the free electrons are trapped). The process is linear in this region, so that the incubation time is given by[39-41]

$$\tau_{\rm inc} = \frac{1}{(2g - \alpha_{\rm l})v} \ln (I_{an}/I_{aT}). \tag{8}$$

Since the beginning of the saturation region is well defined, once we know the incubation time we can estimate the initial nucleation level I_{aT} even when it is of nonthermal origin.

The natural way to investigate the evolution of acoustic instability is to investigate the acoustic flux at the end of the sample, using piezoelectric transducers.[42] This gives the spectrum of the emitted flux and its spectral density, but only at one point, namely, at exit from the sample.

An effective method of investigating this phenomenon is to examine the field distribution along the sample, using ohmic[38,43,44] or capacitive[45] probes. The field in a homogeneous sample is initially constant, but as nonlinear effects set in and the effective electron mobility declines because of the trapping of electrons by the piezoelectric field, the field is redistributed. The redistribution of the electron concentration also has an effect on the field redistribution, and ensures that the potential becomes a nonmonotonic function of distance along the sample. Theory does not predict this effect, but it has been seen experimentally and requires explanation.

A technique exploiting the dependence of the microwave attenuation coefficient on the acoustic flux has also been developed. It was shown theoretically and experimentally[46] that when the electric field vector in the microwave radiation pointed along the wave vector of the acoustic flux, the result was a reduction in attenuation because of reduced effective mobility due to electron trapping.

3.2. Optical methods

These methods have yielded the greatest amount of information about the development of acoustic instability. First, we note the method of induced birefringence in which the Pockels effect produces an additional contribution to n_0 and n_e, so that the beam passing through the sample receives an additional phase shift between the components, which in turn leads to the rotation of the plane of polarization at exit from the sample and to a change in its intensity when it passes through a polaroid. The method is sensitive to the integral flux intensity and can be used to visualize it directly.[47]

The largest amount of information about the development of acoustoelectronic instability was obtained by the Mandel'shtam–Brillouin diffraction[48-50] which we shall now examine in greater detail. The principle of this method is simple. The elasto-optic coefficients ensure that the acoustic wave modulates the permittivity of a transparent sample (there are also other mechanisms, e.g., electron density modulation[51] etc., but these are usually less effective, and need only be taken into account in special cases). For plane waves, scattered light is observed only when the Bragg conditions are satisfied, i.e., when the angle of incidence φ_1 of light (in an isotropic medium) on the acoustic wavefront is equal to the angle of reflection, and the angle of diffraction satisfies the condition $q/2 = k \sin(\vartheta_d/2)$. In the case of a complicated perturbation of the sample, Mandel'shtam–Brillouin scattering can be used to investigate the total spatial spectrum of the perturbation (in its modulus, i.e., at the temporal frequency, and in the direction of q) by varying the angles of incidence and diffraction. It is possible to investigate the time dependence of the spectrum, and its dependence on position can be studied by displacing the probing light beam along the sample.

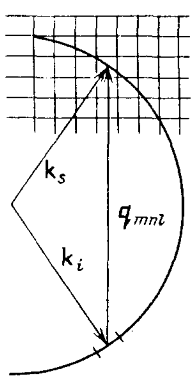

FIG. 8. Scattering of the pump k_i by the component q_{mnl} of the expansion of sound into a spectrum over the cells mnl.

All this is illustrated by the well-known vector diagram shown in Fig. 8 in which the acoustic wave vector q is added to the wave vector k_i of the incident light. The spectral components of the wave vectors q whose end points lie on the Ewald sphere of radius k are active in scattering, and the scattering intensity in each direction is proportional to the intensity of the corresponding component of the wave vector q. Thus, without using time-domain spectroscopic devices, we can deduce from the scattering geometry the modulus of the acoustic wave vector and the temporal frequency, provided we know the type of the scattering wave and the dispersion relation.

The situation is more complicated in birefringent crystals. In the case of interaction with transverse waves, the polarization vector rotates by 90° during diffraction, and instead of 0–0 or e–e isotropic diffraction we have e–0 or 0–e anisotropic diffraction. This is accompanied by a qualitative change in the diffraction geometry.[52–54]

3.2.1. Three-dimensional character of the diffraction process

The Mandel'shtam–Brillouin scattering method is subject to certain limitations[55] that must be borne in mind in the analysis of experimental data, since otherwise errors may creep in. The first of these limitations is imposed by the three-dimensional character of the diffraction. The foregoing discussion was confined to planar diffraction; i.e., all three vectors q, k_i, and k_s (the diffraction triangle) lay in the plane that coincided with the plane of incidence, the exit plane, and the plane of the apparatus. However, the components of nucleating noise can be amplified within a cone drawn around the direction of the draft field.[56] In the planar case, only an infinitesimally thin layer of this cone is accessible to analysis, and most of the spectral components of the amplified flux leave the plane of the apparatus, so that the diffracted beam emerges from this plane.

This means that, to determine the modulus and the direction of the acoustic wave vector in space, we must measure at least three angles, namely, the angle of incidence ϑ_i in the plane of the apparatus, the azimuthal angle ϑ_s, and the position angle α_s of the escaping beam. The basic relationships used in this calculation must be modified accordingly.[57]

However, the three-dimensional character of the diffraction process leads not only to complications in the analysis of experimental data, but also to qualitatively new effects. First, we note when the receiving aperture is a vertical slot (which is often the case in practice), this leads not only to the complete loss of information about the angle of escape, q, from the horizontal plane, but also to uncertainties in the determination of $|q|$ which for small values of $|q|$ can reach a few dozen percent.

Next, while in the planar case, the polarization of the scattered light is unaffected (isotropic diffraction) or rotates through 90° (anisotropic diffraction), these selection rules fail in the general case. The longitudinal wave begins to contribute to anisotropic diffraction and the transverse wave to isotropic diffractions. This removes the degeneracy and multivaluedness of the diffraction process, so that different additional data have to be used to obtain reliable results.

Apart from introducing a second degree of freedom in the detecting device, we have a further possibility in the investigation of the three-dimensional character of the process, namely, we have at our disposal the inclination of the crystal to the plane of the apparatus.[58] The diffraction geometry remains planar in this case, but the inclination of the crystal can be exploited to investigate the inclined components of the acoustic flux as well. The ambiguity in the scattering process is thus removed, and this significantly facilitates the interpretation of the data although numerical calculations are still necessary. However, this method introduces a considerable complication into the design of the system used to move the crystal.

3.2.2. Effect of finite volume

The second restriction on the Mandel'shtam—Brillouin scattering method is imposed by the finite volume of the scattering region.[32,59] Actually, to achieve satisfactory spatial resolution, the probing beams must have a small enough diameter. At the same time, the natural divergence of the focused beam of this type introduces an uncertainty into the determination of the angles; i.e., the scattered wave vector cannot be established with sufficient precision. This is a manifestation of the principle of complementarity at the macroscopic level. Let us examine this in greater detail.

The interaction between the probing light beam and the deviation $\Delta\varepsilon(r)$ of the permittivity from its equilibrium value in the illuminated portion of the sample gives rise to the distribution $p = E(r)\Delta\varepsilon(r)$ of the induced polarization vector that acts as the source of the secondary (scattered) light.[32,33,59] This distribution occupies a finite volume confined to the region of intersection of the probing beam and the crystal. According to the Kotel'nikov–Shannon theorem, the spectrum of any distribution that is limited in space is in principle continuous and infinite and can be represented by a discrete infinite series in sampling functions of the form $\operatorname{sinc} x = \sin x/x$, i.e.,

$$p(q_x, q_y, q_z) = \sum \sum_{-\infty}^{\infty} \sum p(q_{mnl}) \operatorname{sinc} a_1(q_x - 2m\Delta q_{01}) \times \operatorname{sinc} a_2(q_y - 2n\Delta q_{02}) \cdot \operatorname{sinc} a_3(q_z - 2l\Delta q_{03}), \quad (9)$$

where $\Delta q_{0j} = \pi/2a_j$, a_j are the dimensions of the interaction region. Each sampling function in spectral space is analogous to a phonon when mechanical oscillations are resolved into a spectrum, and by analogy with a phonon in real space, each such function has a proper mode associated with it. Accordingly, each mode is in fact an elementary oscillation that can be excited independently. However, not all the modes are active in emission because emission is confined to the phase cells that are cut by the Ewald sphere (Fig. 8). Each active mode in emission corresponds to an elementary beam whose divergence is determined by the effective transverse dimension of the scattering volume. In the far-field zone, these beams come into contact with one another, and fill the entire sphere densely and uniformly (Fig. 9). The intensity of each elementary beam is related to the mode excitation intensity by the universal transfer coefficient. This means that the radiation field emitted by an arbitrarily excited finite scattering volume can be represented by a finite discrete series of elementary sources.

This approach provides us with a means of estimating correctly the possibilities of the Mandel'shtam–Brillouin method and of optimizing the experimental conditions. Actually, there is no point in using an aperture that is smaller

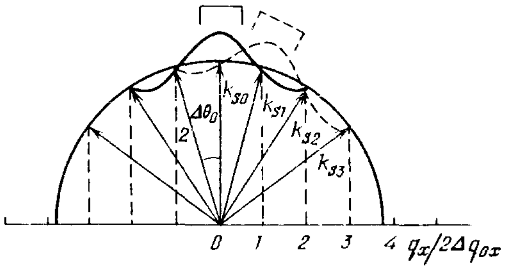

FIG. 9. Subdivision of the spatial spectrum of the source (plane-wave case) into elementary phase cells of size $\Delta q = \pi/2a_j$ and the corresponding subdivision of the resulting field into elementary beams; the true shape of the envelope of the beam is replaced by the equivalent rectangles.[32]

than the diameter of an elementary beam because this would reduce the signal intensity and no new information would be produced. Nor is there any point in using an aperture that is greater than an elementary beam because although this would increase the signal intensity it would also give rise to a loss of resolution. The receiving aperture must therefore be matched to the exit aperture, i.e., to the diameter of the probing beam. The latter is in turn determined by the required spatial resolution which should not exceed 10–100 μm for an experimental gain of the order of 100–1000 dB/cm. We also note that to produce experimental data that can be readily interpreted, the time resolution must be no worse than 25 ns (which is consistent with the time taken by sound to transverse the probing beam). Inadequate temporal resolution and the production of time-averaged data in the rapidly-varying processes that are observed experimentally, means that such data are unsuitable for analysis.

Unfortunately, many workers have ignored these properties of the Mandel'shtam–Brillouin scattering method and this may well be one of the main reason for the spread among the experimental data which must be viewed with considerable caution. The second possible reason for the spread is that the properties of the samples employed depend on the technology used to grow the AIIBVI crystals, which is still relatively inadequate.

3.3. Applications of x-ray scattering

X-rays are used[60] in the analysis of high-frequency acoustic fluxes, especially in the case of opaque crystals such as GaAs. In principle, this is equivalent to Mandel'shtam–Brillouin scattering, but with an extended frequency range. The fundamental disadvantage (apart from technical difficulties) is the low temporal resolution.

3.4. Measurement of the absolute acoustic flux density

The methods described above are suitable mostly for relative measurements. There is, however, considerable interest in absolute intensities as well, but there are no direct methods for measuring the acoustic flux density in the range under consideration. This is so since it is practically impossible to apply this flux to some particular measuring device because of the very high attenuation in acoustic ducts. The flux density must be measured at each point, and this can only be done by indirect methods.

In one of the first methods of this type, the acoustic flux was measured after the field pulse was turned off. Clearly, the current was related to the number of electrons trapped by piezoelectric field, so that the power could be estimated from the Weinreich relation. However, this method is suitable only in the linear or weakly nonlinear situations. In the case of complete electron trapping, the acoustoelectric current carries no information on the flux density (this was confirmed experimentally in Ref. 61).

3.4.1. Measurement of intensity using the Franz–Keldysh effect

The electric field accompanying the elastic wave affects the optical properties of the sample, and this can be used to measure the flux intensity. It is also possible to use the electro-optic effects,[47] but this is inconvenient because they are not single-valued. We shall therefore consider the influence of the piezoelectric field on the band-edge shift due to the Franz–Keldysh effect. It is clear that, in principle, this shift is determined by two factors, namely, the drift field[62] and the piezoelectric field associated with the acoustic flux.[63] It is readily shown that, after saturation, the piezoelectric field due to the acoustic flux is related to the drift field as follows: $E_{1s}^2 = 2en_0\varkappa^2E_0/\alpha_L\varepsilon$. Hence it follows that the contribution of the acoustic flux is predominant for typical concentrations and lattice attenuations. This is seen experimentally as a delay of higher attenuation relative to the field pulse.

Let us now examine this effect in greater detail for real semiconductors whose absorption edge obeys the Urbach rule $\alpha = \alpha_g \exp[-\sigma_F(\omega_g - \omega)]$ where $\sigma_F = B\hbar/k_BT$, α and α_g are the light attenuation coefficients at frequencies ω and ω_g, respectively, and B is the relative steepness. The application of an electric field[64] is equivalent to a band-edge shift by the amount

$$\hbar\Delta\omega = \frac{\hbar^2B^2e^2}{24(k_BT)^2m^*}E^2. \tag{10}$$

The piezoelectric field of an acoustic wave modulates the attenuation coefficient with amplitude $\Delta\alpha_1 = \alpha[\exp I_a/I_{ae} - 1]$, where

$$I_{ae} = \frac{12\varepsilon vm^*}{\hbar^2e^2\varkappa^2}\left(\frac{kT}{B}\right)^3. \tag{11}$$

By measuring the change in the transmitted light intensity and then averaging the attenuation coefficient over the acoustic wavelengths, we can thus determine the acoustic flux density. Since many of the parameters, including the steepness of the Urbach edge, are not usually known to a high precision, we may expect that the total uncertainty in the flux density determined in this way could be of the order of 50%. Although this is not high precision, more accurate methods are unfortunately not available at present. The experiment reported in Ref. 66 was concerned with studying the saturation level by this method, and has confirmed its possibilities by demonstrating agreement with calculations based on (4).

3.4.2. Determination of intensity from excitonic luminescence

We now mention one further method that is essentially an indicator that a particular intensity threshold has been exceeded. We know that a certain fraction of free electrons present in a semiconductor is coupled to holes, forming free excitons, so that an electric field close to the exciton ionization field should produce a reduction in the intensity of excitonic luminescence.[67] In addition, there is also the piezoelectric field of the acoustic wave, which enables us to estimate the flux density. For CdS, the ionization of excitons begins at ~ 30 kV/cm, which corresponds to a flux density of about 10 W/cm^2 (for a longitudinal wave). This effect has been observed experimentally.[68]

4. EXPERIMENTAL RESULTS ON THE DEVELOPMENT OF ACOUSTIC INSTABILITY

We note, first, that in the great majority of published experiments, the development of acoustic instability was observed only for transverse piezoactive T2 waves. This was not unexpected when the field was applied at right angles to the C_6 axis. However, even when the field was applied parallel to this axis, oblique T2 waves (at 30°) were also amplified (instead of the expected amplification of longitudinal waves). This property will be discussed below.

Next, it may be considered as established that there are two fundamentally different amplification regimes, namely, the low-gain regime (approximately 100 dB/cm or less) and the high-gain regime for which nonlinearity is reached after only a fraction of the length of the sample.[69] In the former case, the instability initially develops roughly along the lines predicted by the linear theory, but then, after a few transits, it gives way to a standard domain near the anode. In the latter case, a traveling acoustoelectric domain is formed after only one transit and takes the form of a wave packet in which the sound intensity is much higher than elsewhere in space. Practically the entire applied potential is developed across the domain which moves with velocity close to the velocity of sound. We shall now consider these regimes in greater detail.

4.1. Low-gain regime

This has been investigated by a large number of workers[70] and its main features are now well understood. The process develops as follows. Linear amplification of the nucleating noise begins as soon as the field is applied. The noise distribution function rises monotonically in space and tends to the exponential distribution. At the same time, the acoustic flux begins to be reflected by the anode. For a number of reasons, including a possible change in wave type on reflection,[71] the reflected flux is attenuated to a lesser extent than the corresponding amplification of the incident flux. Repeated reflection by the cathode is therefore found to produce a wave in the forward direction that exceeds the original noise level. This wave is again amplified and the process repeats several times until the flux near the anode reaches the level at which nonlinearity begins; i.e., $e\Phi_1 \sim 0.1 k_B T$. Electrons then begin to be trapped, the effective resistance of the region near the anode rises, and the field in this region increases. In accordance with the theory, the increase in the field produces an increase in gain and an expansion of the dynamic range near the anode as well as a reduction elsewhere. The acoustic flux density at the anode increases as a result of this, but elsewhere it falls until the dynamic equilibrium is reached. At the same time, the flux density at the anode is much greater than elsewhere in the sample. This type of distribution is commonly referred to as an acoustic domain. The development process is well illustrated by a stepped fall in the current through the sample from its ohmic

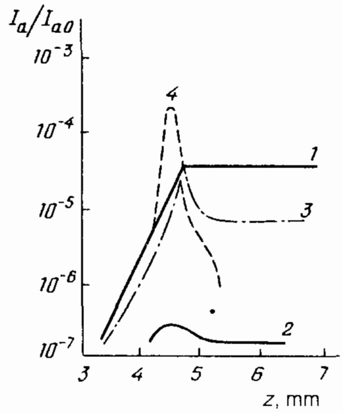

FIG. 10. Flux distribution in CdS without the piezoshock (*1*,*2*) and with the piezoshock (*3*,*4*) at 2.5 GHz (*1*,*3*) and 0.28 GHz (*2*,*4*); $\gamma = 0.38$; $t = 2.6\,\mu$s (Ref. 72).

value prior to saturation. The step length is usually equal to twice the double transit time in the sample.[38]

The real picture is usually only qualitatively similar to the above description because the plateau on the intensity distribution along the sample is not observed even at the initial time. To establish the reasons for this, Gelbert and Many[72] have performed a special experiment in which a double-pulse technique was used to produce a significant reduction in the effect of the piezoelectric shock in the region near the cathode. A subcritical field was initially applied to the sample, and was followed by a further small field pulse after a certain time sufficient for the oscillations in the region of the cathode to die down. The net effect of this was that the resultant field rose above the critical value and the acoustic instability of the thermal level began to develop (Fig. 10). Agreement with theory was reported in Ref. 72 for single-transit conditions. This suggested that the simple model was valid for these particular experimental conditions. This paper is also of major importance because it provides direct experimental confirmation of the importance of shock noise near the cathode in the nucleation process during instability development. We shall return to this question below.

There have also been experiments[73] on the dependence of the velocity of sound on supercriticality as predicted by theory. They showed that for low supercriticalities ($\gamma \ll 1$), the velocity of injected sound depended significantly on frequency and applied field. The agreement with theoretical predictions was found to be adequate.

The parametric interaction between two injected signals and between signal and noise has also been investigated.[74-82] Experiments confirmed the possibility of parametric (including non-Peierls) interaction and have shown that energy can be transferred from one wave to another when the corresponding phase relationships determined by the angle between the directions of propagation are satisfied (low supercriticality and significant dispersion). It was also shown that the parametric signal/noise interaction can lead under certain conditions to the transfer of energy from signal to noise and, eventually, to the suppression of the signal. It was suggested that this was why a practical electric-signal amplifier could not be produced.

There is considerable interest in the spectral composition of a developing instability. In the multitransit regime there is a continuous downward shift of the frequency at maximum spectral density by a factor of two or more.[77,83] It was suggested that this was a consequence of the parametric (mostly degenerate) interaction involving the splitting of the main phonon into two phonons of roughly equal energy. It was shown theoretically that, in the case of weak nonlinearity, this interaction was possible not only for monochromatic signals, but also for noise,[80,81] and that in this approximation the conversion efficiency increased with increasing signal amplitude.[74] The same mechanism was considered in quantum-mechanical language[76] in terms of phonons rather than waves. It was shown that the Peierls interaction (quantum-mechanical analog of the three-wave parametric interaction) and the non-Peierls interaction with the participation of a highly damped electron-density wave (quantum-mechanical analog of the four-wave parametric interaction) could also explain this effect. Finally, it was shown that the non-Peierls interaction was more effective than the Peierls interaction, and that the former was usually employed at present to explain the frequency shift.

However, it is important to emphasize that all theoretical work has been confined to the weak-nonlinearity approximation. It is only in this approximation that the interaction effectiveness increases with increasing wave amplitude. It seems that there is no justification for the extension of the range of validity of this theory to the intermediate nonlinearity regime, which is frequently done in experimental publications. It can be shown that under the conditions of intermediate nonlinearity, the conversion efficiency falls by analogy with the fall in gain (see Fig. 6). For a deep nonlinearity, the fourth-order (non-Peierls) interaction should vanish; i.e., an electron bunch cannot be lost since it is separated from neighboring bunches by high potential barriers.

The reduction in the frequency at maximum spectral density in the case of the multitransit regime can be explained as follows. Gelbert and Many[72] have shown that the down-conversion of frequency is not observed in the single-transit regime for low supercriticalities. Consequently, the reverse propagation of the wave reflected by the anode may well play an important role. Actually, since this wave reaches the cathode, the contribution of electron attenuation is relatively small and lattice attenuation plays the dominant role especially when there is a change in wave type on reflection. This attenuation decreases with decreasing frequency. It follows that low frequencies are emphasized in reverse propagation of the flux, and each transit is accompanied by a downward shift of the spectral density maximum until this is compensated by a reduction in gain in forward transit. The net result of all this is the appearance of a cutoff frequency for the acoustic flux.

4.2.

The development of acoustic instability undergoes a fundamental change under high-gain conditions (gain in excess of 100 dB/cm). The acoustic flux reaches the strong nonlinearity level after a single transit, and this gives rise to a moving acoustoelectric domain (AED).[84,85] The AED is a short (of the order of 100 μm) packet of acoustic oscillations propagating in the sample with the velocity approaching the velocity of sound. The properties of this domain are unusual and do not fit into the framework of existing theories. We begin by listing them.

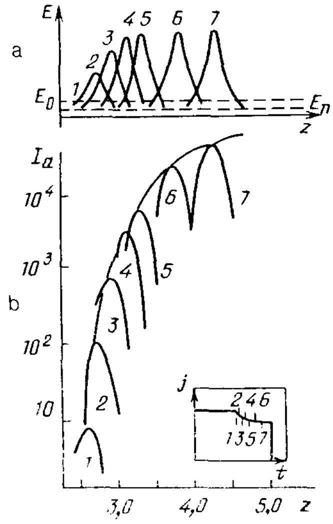

FIG. 11. Acoustic flux (a) and electric field (b) distributions at times 1–7 indicated on the current pulse oscillogram (see insert) during the evolution of a domain (Ref. 86).

4.2.1.

The AED is first recorded after a time approximately equal to the incubation time, i.e., at the onset of an appreciable reduction in current.[86–89] The domain is therefore a definitely nonlinear formation, and its amplification coefficient must fall smoothly with increasing intensity (Fig. 11). This was not observed in the experiment in which the domain was found to grow exponentially or even super-exponentially with gain (by two orders of magnitude in the latter case). It was only after the current reached saturation, i.e., in the region of deep saturation, that the gain began to decrease (Fig. 11). These unusual properties of the nonlinear regime cannot be explained by the theories described above.

4.2.2.

The AED is not formed if the gain is high but the applied field is greater than the optimum value ($\beta_E > 1$). There are few such experiments because high fields are associated with high breakdown probability in the crystal, usually on the surface. However, the authors of Ref. 66, for example, used a high initial electron concentration for which the time taken by the acoustic flux to reach the saturation did not exceed the ionization time of air, and performed their measurements using short field pulses that did not give rise to breakdown in the sample. Their results showed laminar flux growth under these conditions, and a domain was not formed.

4.2.3. Properties of domain propagation velocity

The graph of the position of domain maximum as a function of time shows that, on average, the points lie on a straight line whose slope is close to the velocity of sound.[86,89] When the straight line is extrapolated to $t = 0$, it is found to cut the cathode to within the dimensions of a domain. However, between its point of creation and the point at which the AED reaches saturation, the velocity of the crest of the domain is found to deviate from the velocity of sound, which, in all probability, is related to a change in the domain shape. Careful measurements were performed with a system incor-

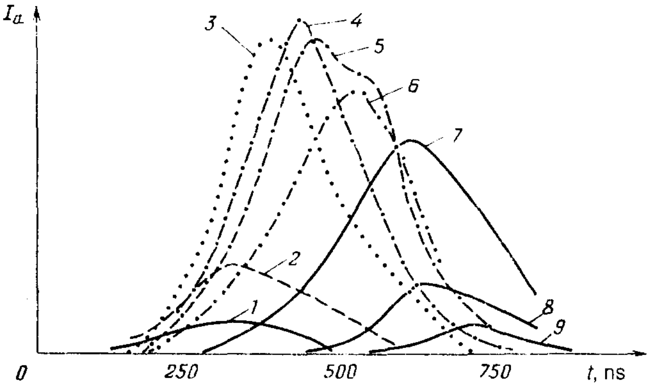

FIG. 12. Acoustic flux distribution vs time for the distance from cathode (1 mm): 1—1.05; 2—1.25; 3—1.45; 4—1.65; 5—1.85; 6—2.05; 7—2.25; 8—2.45; and 9—2.65.

porating multichannel digital storage and recording of the complete temporal profile of the signal at each point, and the resulting data were used to reconstruct the distribution of flux along the sample with time as the parameter. These measurements showed[90] that, on the superexponential growth curve, the leading edge of the domain travelled with velocity close to the velocity of sound (in fact somewhat higher than the velocity of sound) and its crest and trailing edge were practically at rest, but had greater amplitude (Fig. 12). This behavior is consistent with an absolute (rather than convective) flux instability predicted for the acoustoelectronic interaction. We emphasize, however, that the absolute instability is observed not in the linear regime, for which the theory was developed, but in the essentially nonlinear regime.

As the growth in domain intensity slows down, and begins to reach saturation, the domain seems to free itself and begins to move as a whole with velocity close to the velocity of sound.

When the crystal quality is not adequate, or the domain is observed in a longitudinal crystal (oblique T2 waves), a more complicated picture can also be observed: the domains may begin to bifurcate, the first domain may decay and be replaced by another at the same time but at a different point, a double domain may be observed, and so on. In all probability, such effects are due to crystal inhomogeneity and reflections from the side surfaces of the sample. Such complicated situations will not be discussed below.

4.2.4.

The domain length depends on the conductivity of the sample, the applied field, and the crystal type. Detailed measurements of these functions have not been carried out, but the domain length in CdS is usually 100–300 μm. This length tends to its lower limit with increasing conductivity and decreasing field.[47,87]

4.2.5.

The average spectrum of the contents of a domain corresponds to quasimonochromatic noise and its relative width is $\Delta\Omega/\Omega_0 \approx 1/3$, in accordance with the above theory. However, even at the point of domain nucleation, the frequency at maximum is in most cases below Ω_0. As already noted, this is usually explained in terms of three factors, namely, the influence of lattice attenuation, the influence of the initial spectrum of the nucleating shock packet, and the influence of attachment centers.[91,92]

The most interesting and least understood is the behavior of the spectral density maximum during the amplification process. Since the domain is obviously a nonlinear formation, the spectrum may be expected to shift upward as a result of the generation of harmonics.[93] Experiment shows that, in fact, the spectrum shifts smoothly downward within the super-exponential region of domain growth. It then reaches the first subharmonic and usually stabilizes in the region of domain saturation. As in the low-gain case, this shift is usually explained in terms of one-dimensional parametric interactions. However, this explanation is valid only in the region of weak nonlinearity. On the other hand, the observed frequency shift occurs in the intermediate nonlinearity region.

There are also several experiments that do not fit into the theoretical scheme. First, there are the two papers reported in Refs. 94–95 in which the experimental situation is similar, but the results are fundamentally different. Monochromatic sound of appreciable amplitude, generated by an external source, was introduced in these experiments into the amplifying sample, and light scattering was used to observe the change in its spectrum. The frequency of the injected sound was in both cases greater by a factor of 2–3 than the frequency at maximum gain. Intensive generation of subharmonics was observed as usual in Ref. 94, and harmonics were not recorded. On the other hand, Ref. 95 reported intensive generation of harmonics, and the level of subharmonics was much lower. No explanation was offered of this difference, but a possible interpretation is presented below.

Another series of experiments that is in conflict with parametric theories involved studies of instability development in active regions with small transverse cross section. The first of these publications[60] was concerned with x-ray diffraction and reported a study of the spectrum of amplified high-frequency (60 GHz) flux in a thin (20 μm) gallium arsenide film. It was found that the peak of the spectrum occurred at the theoretical value of the frequency at maximum gain, and no subharmonics were observed. This fact was said to be surprising, but no interpretation of it was offered. We note, however, that the single-particle regime ($ql < 1$) and not the hydrodynamic amplification regime ($ql > 1$) was involved in this experiment. It is difficult to believe that the Peirels or non-Peirels phonon interaction mechanisms can operate in this regime in a different way. However, it would be desirable to confirm this under the usual hydrodynamic conditions. In the special experiment reported in Ref. 96, a thin filamentary active channel (diameter 120 μm) was produced in a photosensitive bulk sample of CdS by illuminating it with a collimated pump beam through one of the ends (Fig. 13). It was found (Fig. 14) that a continuous downward shift of the frequency at spectral maximum did not take place in this channel (an abrupt frequency change occurred across any inhomogeneity that randomly entered the channel). On the other hand, an increase in the channel diameter to 200–300 μm was accompanied by a qualitative change in the picture; i.e., as usual, the spectrum shifted into the region of the first subharmonic.

These results demonstrate that the transverse size of the interaction region has a fundamental effect on subharmonic

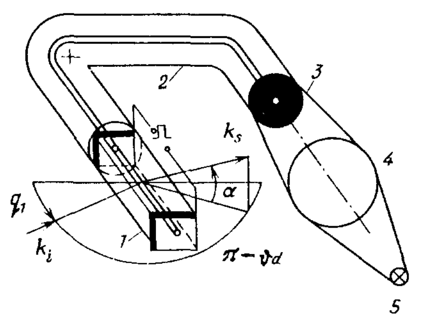

FIG. 13. Experiment with a thin active channel in a sample: 1—sample, 2—lightguide, 3—stop, 4—lens, 5—mercury lamp (Ref. 96).

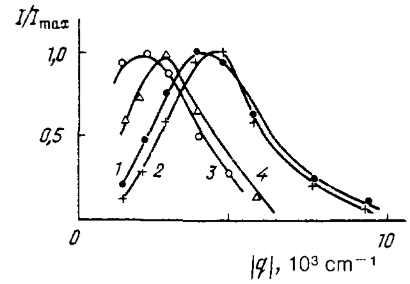

FIG. 14. Acoustic flux spectrum inthe active channel at 2.5 (1), 3.2 (2), 3.4 (3), and 3.8 mm (4) from the cathode (Ref. 96).

generation. This is the basis for concluding that one-dimensional theories are not really valid for real experimental situations, and that steps must be taken to seek an alternative mechanism. In all probability, this mechanism is related to the transverse incoherence of the noise flux, which will be discussed below.

4.2.6.

Interesting results have been obtained by measuring the width of the spatial spectrum for fixed $|q|$ and, in particular, for the frequency at maximum gain. It was found[17] that this width, i.e., the divergence of the corresponding acoustic flux, is usually 5°–10°, which is close to the theoretical value. Hence, it follows that the flux coherence length is of the order of a few wavelengths. The high-frequency wings are smaller in the nonlinear than in the linear region. The entire flux can therefore be represented by a set of contacting coherence tubes for which transitions between the tubes in the nonlinear case are smoother than in the linear case.

Hence it follows (at first sight paradoxically) that the one-dimensional model with infinite plane waves corresponds, typically, to an experiment with a thin active channel and not a thick bulk sample. Actually, if the channel diameter is much greater than the wavelength of sound, waveguide effects are still relatively insignificant and the wave propagates effectively in free space. On the other hand, if the channel diameter does not exceed the flux coherence length, the wave is transversely coherent within the channel, and this corresponds to the one-dimensional theory.

4.2.7.

As noted in Sec. 4.2.5, the relative width of the temporal spectrum of a domain is of the order of 1/3. However, the intensity of light scattered by the domain is usually subject to very strong amplitude fluctuations (by a factor of 10 or more), so that the width of the spectrum is essentially an average over many realizations of this process.

This question was investigated in a special experiment in which the statistical properties of light scattered by a domain were studied as a function of the width of the receiving aperture.[97] The experiment was designed as follows. The scattering geometry was matched to the signal maximum for optimum receiving aperture. A strobe pulse was then used to find the maximum amplitude of light scattered by the domain, which was recorded by a digital multichannel analyzer for each realization (out of a total of 128 realizations). A statistical analysis of the data was then carried out to determine the intensity mean and variance as functions of the size of the receiving aperture. The results are shown in Fig. 15.

It is clear from this figure that the mean intensity at first increases with increasing aperture, but eventually saturates. This behavior is not unexpected: when the receiving aperture is large, all the light scattered by the quasimonochromatic acoustic flux in different directions within the cone defined by the width of the flux spectrum is intercepted by the receiving aperture.

The variance exhibits a much more interesting behavior. At first, and as expected, the relative variance increases as the square root of the signal intensity. However, when the curve turns over and the intensity begins to saturate, the variance at first decreases as the square root of intensity, but eventually tends to a value determined by instrumental noise ($\sim 5\%$).

We must now compare these results with possible models. If we suppose that the spectrum of each realization of a domain is identical with the average, and that the intensity fluctuations are caused by fluctuations in the integral inten-

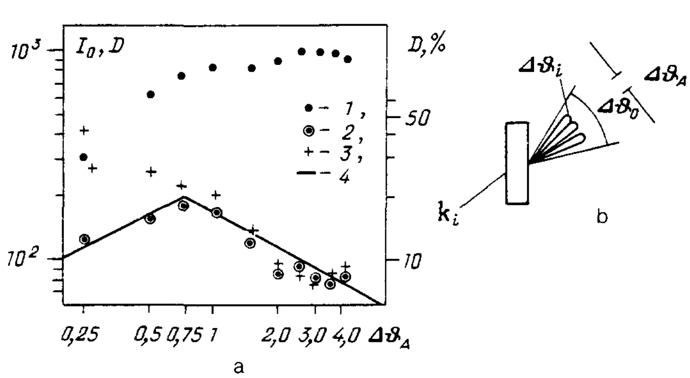

FIG. 15. a—Mean scattered intensity I_0 (1), absolute (2) and relative (3) mean square deviations as functions of the receiving aperture. Points—experimental, curve 4—calculated, normalized to the peak; b—scattering process; $\Delta\vartheta_i$—width of diagram in each realization, $\Delta\vartheta_0$—total width (Ref. 97).

sity of a domain, then the variance should not depend on the size of the receiving aperture. This assumption is in conflict with experimental evidence. The second possibility is that the AED frequency content varies from realization to realization in a random fashion between limits determined by the amplification bandwidth at constant integral AED intensity. This model is in agreement with experiment. Actually, the scattered beam of light in each such realization points in a somewhat different direction (see Fig. 15) and this gives rise to fluctuations in the recorded signal when the aperture is small. As the size of the aperture increases, the signal must fall into the aperture and its variance tends to zero.

This experiment has thus shown that the recorded domain spectrum is usually an average over a large number of realizations. However, the spectrum of an individual realization must be narrower than the average by a factor of at least six. Correspondingly, the coherence length must also be greater, and in each realization the domain is almost completely longitudinally coherent along its entire length. However, the frequency content fluctuates randomly between realizations and within the limits of the amplification bandwidth. This situation cannot occur for a thermal nucleating source, which confirms its shock origin described above.

4.2.8.

Probe measurements of the electric-field distribution in a sample have produced interesting domain data. In high-grade homogeneous samples, the field is initially constant along the entire sample but, as soon as the domain is formed, the field within it begins to rise and rapidly saturates. At this stage, the field reaches its threshold value everywhere except within the domain where it is given by the residual potential divided by the domain length: $E_d = [U - E_t(L - l_d)]/l_t$. This is much greater than the mean field $E_0 = U/L$. This behavior is readily understood: all the electrons are trapped within the domain by the piezoelectric field and travel with the velocity of sound, so that the effective conductivity of the region is lower, which gives rise to a redistribution of the field. Outside the domain, the field is maintained at the threshold value because, in order to maintain the continuity of electric current, the electrons outside the domain must also travel with the velocity of sound.

More detailed and careful measurements of the potential distribution along a sample[89,98-100] have shown that the distribution is not monotonic. A hump and a valley are found to occur in the region of a domain, which clearly shows that an excess charge is stored in the domain, and, often, there is a double layer when the region in front of the domain is depleted. Estimates[89] show that the excess charge amounts to a fraction of a percent of the concentration but, if we recall that the separation between probes used in such measurements is much greater than the Debye screening length, this charge is actually about an order of magnitude greater. For a domain 100–200 μm long, the charge is several times greater than the free-electron concentration as compared with the equilibrium concentration n_0. We know of no explanation of the origin of this charge or of its influence on AED development. However, the charge is expected to play a significant part. We shall discuss this in greater detail below.

4.2.9.

We also note that recent experiments with a thin active channel[96] have revealed the development of longitudinal-wave instability in the longitudinal samples, as expected from one-dimensional theory. In bulk samples, oblique T2 waves, for which the threshold is lower, begin to develop earlier (because of the finite length of the leading edge of the field pulse) and suppress the amplification of longitudinal waves when the nonlinearity region is reached. However, oblique T2 waves propagating in a thin channel will escape from the channel and will not succeed in reaching high intensities. The instability development is therefore found to rely on axial longitudinal waves. This mechanism of suppression of longitudinal waves in bulk samples was put forward long ago, but direct experimental verification has only recently become available.

4.2.10.

These are the basic properties of AED development under high-gain conditions. Some of them can be understood in terms of the generally accepted theory of acoustoelectronic interaction (and examples of this have already been cited), whereas others cannot be so explained. It is clear that the theory of the onset and development of AED must explain all these properties. Unfortunately, papers devoted to the theoretical analysis of acoustic domains have been largely confined to nucleation and, as will be shown below, have not even provided a solution for this problem (let alone the other domain properties).

To begin with, it was suggested that the nucleus of a domain is a shock-wave packet generated in the region near the cathode. Experiments have confirmed this. Moreover, the oscillatory behavior of the process, which has the period L/v for long field pulses, shows that after the shock the cathode region acts as the source of enhanced noise.

Next, it was noted[20] that an inhomogeneous distribution of conductivity along the sample and inhomogeneous illumination may also lead to a domain-like regime. However, in all probability, this can facilitate the evolution of a domain from the nucleating packet, but cannot be the main reason for its appearance.

We also note the paper by Haydl[87] that reports an attempt to explain the single domain structure (SDS). According to Haydl, the SDS appears during the acoustoelectronic instability even for low flux amplitudes. A more rigorous theoretical analysis of this process has shown[2] that the SDS does not occur for low intensities, and this was confirmed by measurements of instantaneous current-voltage characteristics.[101]

Ridley and Wilkenson[19] have examined the evolution of a domain by investigating the nonlinear coupling between space charge and acoustic modes by the Bogolyubov–Krylov method. They succeeded in showing that a domain-like solution was possible in the multimode state in the random-phase approximation. However, this theory does not actually predict any of the domain properties observed experimentally.

Some interesting ideas on the formation and development of a domain can be found in the paper[102] by Butler, but they are not sufficient to explain the properties of a domain.

We therefore conclude that there is at present no final theory capable of explaining adequately the basic properties of a domain. Moreover, it is still not finally clear which physical mechanisms have to be taken into account in domain theory. It follows from experimental data described above, especially the more recent data, that at least three factors are of fundamental importance in the theory, namely, the three-dimensional character of the process, its properties at intermediate nonlinearity, and the accumulation of excess charge in a domain. The development of a three-dimensional nonlinear theory of this kind is found to encounter difficulties that cannot be overcome at present. We shall therefore confine ourselves to a qualitative model of AED evolution and will try to reinforce it wherever possible with numerical estimates.

4.2.11.

Experiment shows that a domain originates in a piezoelectric shock in the cathode region.[72] The amplitude of this wave packet is several times greater than the equilibrium thermal noise level, which is indicated by the fact that the domain incubation time is close to the value obtained numerically for the thermal nucleating noise. This can be explained by the relatively long leading edge of the field pulse and the associated low efficiency of shock excitation.

We may therefore conclude that the initial stage of AED development (which is usually not observed experimentally) can be pictured as follows (Fig. 16). The application of the drift-field pulse gives rise in the cathode region to a relatively long acoustic wave packet which begins to be amplified together with the uniformly distributed thermal noise. In the linear region, i.e., within 5–6 orders of magnitude, the two are amplified independently. The distribution shapes remain the same. The distribution maximum, i.e., the crest of the nucleating wave packet, eventually reaches the beginning of the intermediate nonlinearity region, and at this point the piezoelectric field traps about 10% of the electrons, as indicated by the decay of the current. This is also the beginning of the field redistribution that gives rise to an increase in the field within the domain. If, as is usually the case, the applied field strength is less than the optimum, the increase in the field should lead to higher gain, as already noted.[22,103,104] However, this is opposed by the nonlinear reduction in gain, and it is not clear *a priori* which of these two effects will predominate.

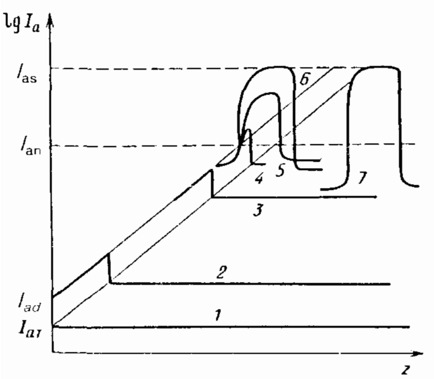

FIG. 16. Simplified model of domain evolution. Acoustic flux distribution at times *1–7*. I_{at} and I_{ad}—thermal and shock nucleation; I_{an}—onset of nonlinearity, I_{as}—saturation.

4.2.12.

Let us examine this process in greater detail on the basis of the results reported by Tien.[20] Suppose that a short acoustic wave packet of length l_d propagates in a sample of length L. The effective conductivity in the region of the packet (in Tien's notation) is given by

$$\sigma_{\text{eff}} = \sigma_0 \frac{y_0}{y}\left[1 - \frac{(1-y^{-1})}{\gamma_d}\frac{r}{p}\right], \tag{12}$$

where $r = 2[1 - (j_s/j)]/x\gamma_0$ is the normalized current saturation factor, $p = 3\beta_E/x$ is the normalized supercriticality, and $y = \gamma + 1$, $y_0 = \gamma_t + 1 = E_0/E_t$.

When this change in resistance is taken into account, we obtain the expression for the field in the region of the wave packet. In the approximation defined by $Lr/l_d p \gg 1$, which is well satisfied in practice, we can readily show that the domain field is

$$E_d = E_0 Lr/l_d p. \tag{13}$$

We can use this expression whenever the reduction in the current is greater than 5%.

We have used these considerations in numerical calculations. The dependence of r on the acoustic flux density was taken from the graphs given in Ref. 20 and the calculation was based on the iteration method described in Ref. 28. The final result is shown in Fig. 17 for a number of selected parameter values. Although, for these values, curves 2–5 are qualitatively similar, physical considerations suggest that curve 3 is closest to reality. It follows from this that, when $e\Phi_1/k_B T \sim 1$, the gain rises by a factor of 2 which corresponds to the super-exponential growth of the domain in the intermediate nonlinearity regime. Since this is accompanied by a reduction in the field outside the domain, the result is a reduction in gain and in the final analysis a complete damping out of the background surrounding the domain. This is why we may consider that the domain evolves from a nucleating wave packet at the beginning of intermediate nonlinearity and after the incubation time following the application of the field pulse. The region with superlinear gain extends up to $e\Phi_1/k_B T \sim 3$. The amplitude rises by a factor

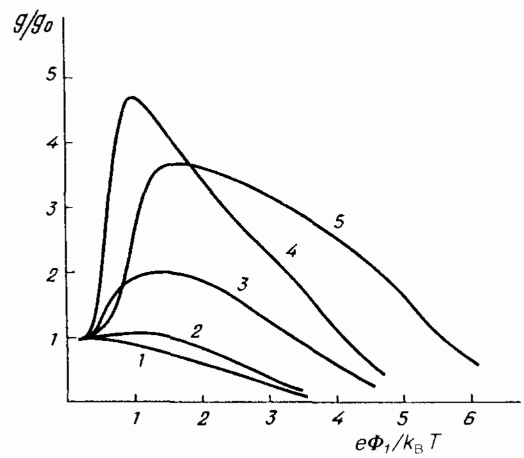

FIG. 17. Relative amplification in a domain as a function of reduced amplitude $e\Phi_1/k_B T$ for different initial supercriticalities and ratios l_d/L: $l_d = 0$; $\beta_E = 0.5$ (*1*); $l_d/L = 0.02$, $\beta_E = 0.5$ (*2*); $l_d/L = 0.2$, $\beta_E = 0.2$ (*3*); $l_d/L = 0.02$, $\beta_E = 0.1$ (*4*); $l_d/L = 0.1$, $\beta_E = 0.1$ (*5*) (Ref. 28).

of 6 over this segment, and this corresponds to an increase in the dynamic range by just over an order of magnitude (in intensity). This result is less than the experimentally observed value which is usually close to two orders of magnitude.

4.2.13.

The field redistribution is accompanied by the onset of charge redistribution.[28] Let us examine this in greater detail.

If the amplitude of the acoustic wave remains constant all over the sample, then it is clear that in the nonlinear regime the electrons can be redistributed only within each wavelength; i.e, all the electrons concentrate near the potential minimum and the average concentration in this half-wave is doubled. It is precisely this case that is considered in all publications.

A different situation occurs in the case of a short acoustic pulse. In the hydrodynamic approximation that we are considering ($ql < 1$), the electrons tend to equalize the distribution and flow into the potential well not merely from the neighboring crest, but also from the entire sample. Accordingly, their mean local concentration in the well is approximately $e\Phi_1/k_B T$ (the volume of the well in units of $k_B T$). However, this filling of the well and the increase in the local concentration continue until the electrons outside the pulse can overcome the potential hill and become trapped in the well. If the height of the crest is $3k_B T - 4k_B T$, the probability that an electron will cross the crest becomes very small and the flow of electrons into the well ceases almost completely. Further increase in the wave amplitude will then not produce a rise in the number of electrons in the potential well, and we may assume in approximate calculations that, for a short pulse, the maximum rise in the number of electrons in the well will be greater by a factor of 3–4 as compared with the corresponding number for a continuous wave. The concentration excess can produce a corresponding increase in the saturation level, and this has actually been observed experimentally[66] and is briefly described in the next section.

There is also a second factor that prevents the accumulation of electrons in the well, namely, the Coulomb field of electrons already trapped in the well (we recall that the amounts of positive and negative piezoelectric charges are equal; i.e., the acoustic packet as a whole is electrically neutral). Under normal conditions, this factor does not prevent the accumulation of charges within one period of the wave and determines the number of waves in the packet in which the accumulation of electrons can take place.

As already noted, the field in a domain is $E_d \gg E_0$ (Fig. 18). The accumulation excess charge ΔNe produces a field whose maximum strength on the domain boundary is $E_e = \Delta Ne/2\varepsilon$. Outside the domain the field decays within the Debye length. It follows that it is only for $E_d > E_e$ that the electrons can still succeed in entering in the domain and be trapped there by piezopotential wells (we are, of course, neglecting the tunnel effect). Since we have already calculated the maximum charge that can be stored in one period, we can use this inequality to determine the total possible domain length:

$$l_d = (\varepsilon U/4en_0)^{1/2}. \tag{14}$$

If we suppose for the purposes of an estimate that $l_d = 100$

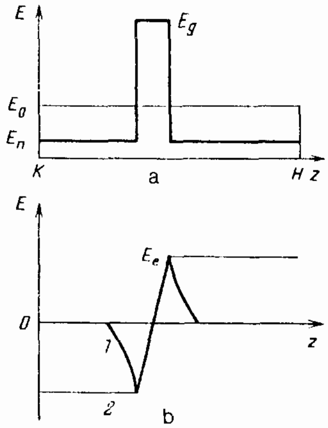

FIG. 18. Field distributions in the sample: domain regime, external field (a) and field due to excess charge in the domain (b) with (*1*) and without (*2*) shielding (Ref. 28).

μm, $L = 10$ mm, and $E_0 = 2$ kV/cm, we find that the maximum excess charge in a domain is $\Delta N = 2 \times 10^{12}$ cm^{-3}, which can produce an increase in the concentration in the domain by a factor of several times. Correspondingly, the dynamic intensity range can expand by roughly an order of magnitude. Since the field and charge redistributions proceed independently, their combined effect should extend the dynamic range by roughly two orders of magnitude, which is consistent with experiment. At the same time, the gain does not in general remain constant in this range and exceeds the linear value by a factor of about 2.

It is readily seen that the domain length l_d that we have obtained corresponds to 15–30 oscillations. Since this is close to the unaveraged flux coherence length indicated by the above statistical experiments, each domain realization is almost completely longitudinally coherent.

4.2.14.

We now return to the evolution of AED from the nucleating wave packet, taking into account the above field and charge redistributions and their effect on the amplification process (Fig. 16). We have already noted that, some time during the amplification of the nucleating packet and thermal noise, the leading edge will reach the beginning of the intermediate nonlinearity region (see Fig. 10). This will mark the beginning of the field and charge redistributions which will lead to the beginning of the field and charge redistributions which will lead to the super-exponential growth of both the leading edge of the domain and the portion behind it. The leading edge will continue to move with the velocity of sound until it reaches the saturation level (see Fig. 12). While all this is happening, the rest of the nucleating packet remains well below the saturation level and is amplified with a high gain. In our coarse approximation, the domain tends to become rectangular, and this is seen experimentally as the motion of the leading edge with the trailing edge pinned down, i.e., as an essentially absolute instability. The process can continue until the entire accumulated charge limits the domain length. The rear wall of the domain then begins to move, and this is seen as the unpinning of the domain from its point of creation, and as the motion of the domain as a whole with the velocity of sound.

The above semiquantitative discussion of the evolution of an AED from a nucleating wave packet is very approximate, but it does account for the main features of domain behavior. Actually, this approach can explain the temporal behavior of a domain, including its creation after the incubation time following the passage of the leading edge of the field pulse, its velocity anomalies, and the reason why the extrapolated curve cuts the cathode. An analytic expression for the domain length was thus obtained for the first time and the result it predicts is close to the experimental value without involving any adjustable parameters. An explanation has also been provided for the super-exponential growth of the domain in the nonlinear regime within a range covering about two orders of magnitude. The reason for the accumulation of excess charge in the domain becomes clear, as is the role played by this charge. The reasons for the fluctuations in scattered-light intensity and the observed spectral width due to averaging have also become clear.

4.2.15.

The shift of the spectrum into the subharmonic region is essentially the only remaining unexplained question. As already noted, the nucleating wave packet is incoherent in the transverse coordinate and is distributed over a large number of practically parallel coherence tubes with diameters of a few dozen wavelengths. Although the packet reaches the level corresponding to the onset of intermediate nonlinearity, the piezopotential humps begin to limit the mobility of electrons in the longitudinal direction without affecting it in the transverse direction.[28] Electron bunches can move freely in the transverse direction under the influence of both Coulomb and diffusion forces. This transverse motion takes the electrons from the region of the potential barrier in one of the coherence tubes into the valley of a neighboring tube. They can subsequently return to the original tube, but only to a previous valley (Fig. 19). This "snaking" of the electrons can continue because of flux incoherence until the piezopotential humps accidentally coincide in neighboring tubes.

It is readily seen that this motion produces an increase in the spatial period of the electron-density wave because the electrons accumulate only on certain piezopotential humps. If the frequency content of neighboring coherence tubes can lie within the amplification bandwidth, i.e., $0.7\Omega_0T$–$1.3\Omega_0T$, the smallest spatial period of sound for which the piezopotential humps can coincide for neighboring coherence tubes is the largest spatial period of sound (Fig. 19). Since the amplification process is local, the only oscillations that will be amplified will be those for which the electrons are found to bunch, and all others will be damped out. This will lead, first, to a reduction in the mean flux frequency by a factor of about 2; i.e., it will shift towards the lower limit of the amplification bandwidth; and, second, the transverse coherence of the flux will increase; i.e., transitions between neighboring tubes will become less sharp. As noted above, both these effects have been observed experimentally.

This mechanism provides a natural explanation not only of the frequency shift itself, but also of its confinement to the intermediate nonlinearity region with the super-exponential domain growth. It is readily seen that this mechanism will not operate either in the linear or the deep saturation regions, but it will explain all other properties of spectrum conversion. Indeed, only the experiments reported in Refs. 94 and 95, in which sound was injected from outside, require special examination. These experiments were found to produce different results, probably because of the special features of the external injection of sound (in so far as we can judge, all the other experimental conditions were the same). We know that a large-diameter source was employed in Ref. 95, so that the sample intercepted a practically homogeneous plane wave. The peripheral regions, in which the wave intensity may have been lower and the relative importance of noise greater, were only of minor importance. Accordingly, "snaking" motion was practically impossible, which ensured the efficient generation of harmonics and the poor generation of subharmonics. We note that the frequency at maximum gain was found to occur in the subharmonic region. The design of the source used in Ref. 94 is not known, but we may suppose that it actively excited only the central portion of the sample. There was therefore very little contribution due to noise from the periphery of the beam, and this assured the efficient generation of subharmonics while completely suppressing harmonic generation.

The snaking motion of electrons described above is thus seen to provide a qualitative explanation of all experiments involving frequency conversion in the subharmonic region. However, a quantitative theory based on this mechanism is still lacking.

5. RESONANCE EFFECTS IN THE ACOUSTOELECTRONIC INTERACTION

Resonance effects accompanying the development of the acoustoelectronic instability are particularly interesting.[67,69,105-110] There are at least two types of effect: One of them occurs in photosensitive crystals in which carriers are

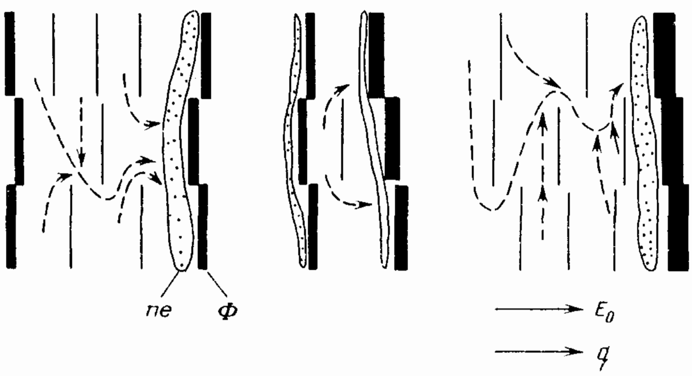

FIG. 19. Distributions of the maxima of piezopotential and number of electrons (schematic). Line thickness is an approximate measure of the potential amplitude and the thickness of the layer of electrons represents their number. Dashed lines show the snaking motion of electrons in a flux consisting of three coherence tubes.

excited by photons whose energies are less than the band gap; the other occurs when the energy of the probing photons is less than the band gap. We shall now consider these very different effects in turn.

We recall at this point that a change in the frequency of light is accompanied by a change in the absolute values of the elasto-optic coefficients,[11] some of which increase and some decrease at resonance. Next, there is also a change in the absolute values of the refractive indices n_0 and n_e. They become comparable near resonance (at the isotropic point[112]) after which the difference between them changes sign and the crystal becomes negative instead of positive. Finally, in real semiconductors, the band edge is not perfectly sharp and obeys the Urbach rule.

5.1. Resonance between probing beam and band gap

We assumed in the foregoing discussion that the modulation of permittivity by an elastic wave was almost entirely due to elasto-optics. There are, however, other modulation mechanisms as well. The most important of these in a piezosemiconductor is band edge modulation by the Franz-Keldysh effect. This is equivalent to an increase in the attenuation coefficient, i.e., modulation of the imaginary part of permittivity. In accordance with the Kramers–Krönig principle, the change in the imaginary part of permittivity leads to a change in the real part, i.e., to the formation of a spatial phase grating which scatters light simultaneously with the scattering due to the elasto-optic constants. This problem is examined theoretically in Ref. 108.

The basic properties of this type of scattering can be summarized as follows. First, the phenomenon exhibits resonance and can be observed only when the frequency of the probing light beam falls on the Urbach edge. Second, since the Franz–Keldysh effect is even, the spatial period of the grating produced by this effect is greater by a factor of 2 as compared with elasto-optics, and scattering occurs as if it were due to the second harmonic of the flux frequency. This produces a radical change in diffraction geometry. Third, whatever the type of the amplified wave, scattering by this mechanism can only be isotropic. Finally, the scattered intensity is not a linear function of the flux intensity: the relation is quadratic (for low intensities) or exponential (at high intensities). Scattering due to the Franz–Keldysh effect is significantly different from scattering due to the elasto-optic effect, and this enables us to separate their contributions experimentally. Experimental results[109] are in reasonable agreement with the theory.

5.2. Properties of the process at almost resonant photoexcitation

When the sample is photosensitive and free electrons are excited almost resonantly by a light beam, it is found that several properties appear in the course of instability development. If the equilibrium concentration of electrons, determined by the attenuation coefficient and pump intensity, is high enough, the saturation of the acoustic flux will also occur at a high level. The piezoelectric field of the flux will produce an increase in the attenuation coefficient as a result of the Franz–Keldysh effect, which in turn will give rise to an increase in the electron concentration. This will produce a rise in the saturation level, and the attenuation coefficient will increase still further. The process forms an avalanche that is not limited by the nonlinearity of the acoustoelectronic interaction factor or lattice attenuation. It follows that resonant photoexcitation gives rise to a new mechanism for the development of acoustoelectronic instability, which leads to a rapid rise in the flux intensity above the usual saturation level. The new saturation level is determined by the fact that the Mott transition[112,113] occurs and high-density neutral plasma bunches are produced when the electron concentration exceeds the critical value ($n_c \sim 10^{18}$ cm^{-3}). These bunches are unaffected by the drift field and do not therefore contribute to amplification. Moreover, they are dragged by the deformation potential and provide an additional damping that rapidly stops the avalanche growth.

This process has been observed experimentally.[66,68] A powerful laser beam was introduced through one end of the sample and acted both as a pump and a probing beam for the observation of back scattering. It was found (Fig. 20) that when the pump photon energy was significantly lower than the band gap, the scattered intensity was a linear function of the drift field. Moreover, the absolute acoustic flux intensity was found to be in good agreement with the theoretical prediction.

When the pump was close to resonance, the acoustic flux intensity rose rapidly by approximately two orders of magnitude and then quickly reached its saturation level. Simultaneous observations of the luminescence spectra showed that, as the flux reached the saturation level, the luminescence spectrum acquired a new and rapidly growing Q-band with a maximum at 505 nm, which is usually interpreted as luminescence of high-density plasma.[115]

The linear theory of the onset of this avalanche growth, developed in Ref. 116, predicts a threshold that is close to the experimental value, which can probably be regarded as a verification of the proposed mechanism.

We note that a similar effect is considered in the theoretical paper by Sitnikov and Shkerdin.[10] The only difference is that, in the latter case, the band edge was assumed to be perfect and the band modulation due to the deformation potential and not the Franz–Keldysh effect. Estimates show that at frequencies typical for the acousto-electronic instability, the contribution of the former mechanism is small as compared with the contribution of the Franz–Keldysh effect, and has therefore not been detected experimentally as yet. We note in conclusion that the initial experimental and theoretical research into the resonant interaction has al-

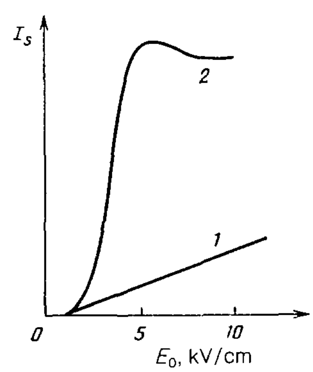

FIG. 20. Scattered-light intensity as a function of electric field in CdS for λ_i = 539.5 (1) and 500.8 nm (2), T = 62 K (Ref. 66).

ready been revealed new and exceedingly interesting aspects of the effect, so that further theoretical and experimental studies are clearly necessary.

CONCLUSION

It is clear from the foregoing presentation that acousto-electronics generally and the development of the acousto-electronic instability in particular are of considerable scientific and practical interest. Many of the problems in this field have long been solved, and have been surveyed in the review literature,[2-7] while other problems were tackled relatively recently and our review was largely focused upon them. Nevertheless, many unanswered questions remain and await a complete solution. Although the new mechanisms proposed recently may well produce a significant contribution to the acousto-electronic interaction, and provide a qualitative explanation of practically all experimental data, the absence of an adequate theory of these processes means that we cannot consider the problem to be fully solved, which is an obstacle to the planning of further experiments and thus tends to delay them. Satisfactory experimental techniques are now available, but there is a lack of high quality samples which are essential if reliable and reproducible results are to be obtained. A technology for growing such samples is still lacking.

The final solution of the problem will have to await the advent of a three-dimensional nonlinear theory of the acousto-electronic interaction for short pulses and the availability of high-grade samples.

[1] A. R. Hutson, I. H. McFee, and D. L. White, Phys. Rev. Lett. 7, 237 (1961).
[2] V. L. Gurevich, Fiz. Tekh. Poluprovodn. **2**, 1557 (1968) [Sov. Phys. Semicond. **2**, 1299 (1968)].
[3] J. H. McFee, "Transmission and amplification of acoustic waves in piezoelectric semiconductors," in *Physical Acoustics*, ed. by W. P. Mason, **4A**, Academic, N.Y., 1966 (Russian transl., Mir. M., 1969, p. 13).
[4] N. I. Meyer and M. H. Jorgensen, Festkörperprobleme, **10**, 21 (1970).
[5] H. Kuzmany, Phys. Stat. Sol. **25**, 9 (1974).
[6] V.I. Pustovoĭt, Usp. Fiz. Nauk **77**, 257 (1969) [Sov. Phys. Usp. **12**, 105 (1969)].
[7] W. Westera, Physica BC **113**, 149 (1982).
[8] J. H. May, Proc. IEEE **53**, 1465 (1965).
[9] D. L. White, J. Appl. Phys. **33**, 2547 (1962).
[10] A. R. Hutson and D. L. White, *ibid.* 40
[11] A. R. Hutson, Phys. Rev. Lett. **9**, 296 (1962).
[12] V. L. Gurevich, Fiz. Tverd. Tela **4**, 909 (1962) [Sov. Phys. Solid State **4**, 668 (1962)].
[13] V. L. Gurevich, Zh. Eksp. Teor. Fiz. **46**, 354 (1964) [Sov. Phys. JETP **19**, 242 (1964)].
[14] S. V. Gantsevich, V. L. Gurevich, and R. Katilyus, Zh. Eksp. Teor. Fiz. **59**, 533 (1970) [Sov. Phys. JETP **32**, 291 (1971)].
[15] Yu. Gulaev, Phys. Lett. A**30**, 260 (1969).
[16] Yu. V. Gulyaev, Fiz. Tverd. Tela **12**, 415 (1970) [Sov. Phys. Solid State **12**, 328 (1970)].
[17] D. L. Spears, Phys. Rev. B **2**, 1931 (1970).
[18] Yu. V. Ilisavavskiĭ and L. A. Kulakova, Fiz. Tverd. Tela **16**, 3417 (1974) [Sov. Phys. Solid State **16**, 2214 (1974)].
[19] B. K. Ridley and J. Wilkinson, J. Phys. C **2**, 1299 (1969).
[20] P. K. Tien, Phys. Rev. **171**, 970 (1969).
[21] V. L. Gurevich and B. D. Laikhtman, Zh. Eksp. Teor. Fiz. **49**, 960 (1965) [Sov. Phys. JETP **22**, 668 (1966)].
[22] V. L. Gurevich, *Proceedings of the 9th International Conference on Semiconductor Physics* [in Russian], Nauka, M., 1968, p. 943.
[23] P. K. L. Gay and H. L. Hartnagel, J. Phys. D **3**, 736 (1970).
[24] A. K. Ganguly and E. M. Conwell, Phys. Lett. A **29**, 221 (1969).
[25] L. A. Chernozatonskiĭ, Fiz. Tekh. Poluprovodn. **15**, 1823 (1981) [Sov. Phys. Semicond. **15**, 1089 (1981)].
[26] B. Weinreich, Phys. Rev. **104**, 321 (1956).
[27] M. Pomerantz, Proc. IEEE **53**, 1388 (1965).
[28] V. M. Rysakov, *Development of Coherence and Domains in Acoustic Fluxes during Instability Development* [in Russian], Preprint from FTI AN SSSR, No. 122, Leningrad, 1988.
[29] V. M. Rysakov, Akust. Zh. **36**, 180 (1990) [Sov. Phys. Acoust. **36**, 101 (1990)].
[30] S. A. Akhmanov, Yu. E. D'yankov, and A. S. Chirkin, *Introduction to Statistical Radio Physics* [in Russian], Nauka, M., 1981, pp. 287 and 297.
[31] I. L. Klyukach and R. I. Sokolovskiĭ, Zh. Eksp. Teor. Fiz. **71**, 424 (1976) [Sov. Phys. JETP **44**, 223 (1976)].
[32] V. M. Rysakov, *Diffraction and Scattering of Light by Phase Gating of Arbitrary Coherence, Application of the Kotel'nikov–Shannon Theorem in the Analysis of these Processes* [in Russian], Preprint from FTI AN SSSR, No. 1108, Leningrad, 1987
[33] V. M. Rysakov and Yu. V. Aristov, Opt. Spektrosk. **63**, 1325 (1987) [Opt. Spectrosc. (USSR), **63**, 785 (1987)].
[34] A. Many and U. Gelbert, Appl. Phys. Lett. **19**, 192 (1971).
[35] T. Ogawa, Jpn. J. Appl. Phys. **9**, 281 (1970).
[36] S. V. Gantcevich, V. L. Gurevich, V. D. Kagan, and R. Katilius, Phys. Stat. Sol. **75**, 407 (1976).
[37] R. K. Smith, Phys. Rev. Lett. **9**, 281 (1970).
[38] I. Yamashita, T. Ishiguro, and T. Tanaka, J. Appl. Phys. **4**, 470 (1965).
[39] R. Bray, C. S. Kumar, J. B. Ross, and P. O. Silva, J. Phys. Soc. Jpn. **21**, 483 (1966).
[40] N. I. Meyer and E. Mosekilde, Phys. Lett. **24A**, 155 (1967).
[41] H. Preier, J. Appl. Phys. **42**, 202 (1971).
[42] J. H. McFee, *ibid.* **34**, 1548 (1963).
[43] J. H. McFee and P. K. Tien, *ibid.* **37**, 2754 (1966).
[44] W. H. Haydl, Appl. Phys. Lett. **10**, 36 (1967).
[45] A. Ishida and Y. Inushi, J. Phys. Soc. Jpn. **25**, 443 (1968).
[46] H. Hess and H. Kuzmany, J. Phys.C **6**, 657 (1973).
[47] A. R. Moore, Appl. Phys. Lett. **13**, 126 (1968).
[48] V. L. Gurevich and V. D. Kagan, Zh. Eksp. Teor. Fiz. **47**, 1782 (1964) [Sov. Phys. JETP **20**, 1201 (1965)].
[49] J. Zucker and S. Zemon, Appl. Phys. Lett. **9**, 398 (1966).
[50] Yu. V. Galyaev, V. V. Proklov, and G. N. Shkerdin, Usp. Fiz. Nauk **124**, 61 (1978) [Sov. Phys. Usp. **21**, 29 (1978)].
[51] W. Wonneberger, F. Siebert, and W. Wettling, Opt. Comm. **3**, 171 (1971).
[52] R. W. Dixon, IEEE J. **3**, 85 (1987).
[53] L. L. Hope, Phys. Rev. **166**, 883 (1968).
[54] N. Wakatsuki, N. Chubachi, and K. Kikuchi, Jpn. J. Appl. Phys. **13**, 1745 (1974).
[55] V. M. Rysakov and Yu. Aristov, Zh. Tekh. Fiz. **56**, 750 (1986) [Sov. Phys. Tech. Phys. **31**, 452 (1986)].
[56] V. I. Pustovoĭt and L. A. Chernozatonskiĭ, Fiz. Tekh. Poluprovodn. **6**, 1311 (1972) [Sov. Phys. Semicond. **6**, 1147 (1973)].
[57] Yu. V. Aristov and V. M. Rysakov, Opt. Spektrosk. **57**, 662 (1984) [Opt. Spektrosc. (USSR) **57**, 402 (1984)].
[58] M. Sanja, M. Yamada, C. Hamaguchi, and J. Nakaj, Jpn. J. Appl. Phys. **13**, 611 (1974).
[59] V. M. Rysakov and Yu. V. Aristov, Opt. Spektrosk. **62**, 850 (1987) [Opt. Spectrosc. (USSR) **62**, 507 (1987)].
[60] D. G. Carlson, A. Segmuller, E. Mosekilde, H. Cole, and G. A. Armstrong, Appl. Phys. Lett. **18**, 330 (1971).
[61] E. P. Garshka, V.I. Samulionis, B. P. Ketis, and A. S. Zhyulpa, Fiz. Tverd. Tela **10**, 611 (1968) [Sov. Phys. Solid. State **10**, 480 (1968)].
[62] A. Ishida and Y. Inuishi, J. Phys. Soc. Jpn. **29**, 679 (1970).
[63] K. Yamamoto, M. Yamada, and K. Abe, *ibid.* **29**, 1251 (1970).
[64] B. O. Seraphin and N. Bottka, Phys. Rev. **139**, 560 (1965).
[65] V. M. Rysakov and Yu. V. Aristov, Fiz. Tverd. Tela **27**, 3413 (1985) [Sov. Phys. Solid State **27**, 2055 (1989)].
[66] L. L. Akatov, Yu. V. Aristov, and V. M. Rysakov, *ibid.* **25**, 1517 (1983) [**25**, 872 (1983)].
[67] D. F. Blossey, Phys. Rev. B **2**, 3976 (1970).
[68] L. L. Akatov and V. M. Rysakov, Fix. Tverd. Tela **23**, 3343 (1981) [Sov. Phys. Solid State **23**, 1941 (1981)].
[69] H. Ozaki, Jpn. J. Appl. Phys. **10**, 804 (1971).
[70] P. O. Silva and R. Bray, Phys. Rev. Lett. **14**, 372 (1965).
[71] E. D. Palik and R. Bray, Phys. Rev. B **3**, 3307 (1971).
[72] U. Gelbert and A. Many, *ibid.* 7, 2713 (1973).
[73] A. M. D'yankonov and Yu. V. Ilisavskiĭ, Pis'ma Zh. Eksp. Teor. Fiz. **7**, 6 (1968) [JETP Lett. 7, 3 (1968)].
[74] S. Zemon and J. Zucker, IBM J. Res. and Develop. **13**, 494 (1969).
[75] A. M. D'yakonov, Yu. V. Ilisavskiĭ, and L. A. Kulakova, Fiz. Tverd. Tela **14**, 2612 (1972) [Sov. Phys. Solid State **14**, 2259 (1972)].
[76] V. L. Gurevich, V. D. Kagan, and B. D. Laitkhman, Zh. Eksp. Teor. Fiz. **54**, 188 (1967) [Sov. Phys. JETP **54**, 102 (1968)].
[77] B. K. Ridley, Phys. Stat. Sol. **48**, 149 (1971).
[78] R. Manro and W. C. Wang, Phys. Rev. B **1**, 683 (1970).
[79] E. M. Conwell and A. K. Ganguly, *ibid.* **4**, 2325 (1971).
[80] B. K. Ridley, J. Phys. C **6**, 1605 (1973).

[81] B. Shapiro, Phys. Rev. B **12**, 2402 (1975).
[82] H. H. Spector, J. Phys. (Paris) Coll. C 6, **42**, Suppl. 12, 676 (1981).
[83] S. Zemon and J. Zucker, Proc. IEEE **56**, 778 (1968).
[84] I. Yamashita, T. Ishiguro, and T. Tanaka, J. Appl. Phys. **4**, 470 (1965).
[85] W. H. Haydl and C. F. Quate, Phys. Lett. **20**, 463 (1966).
[86] W. Wetling and M. Brunn, Phys. Status Solidi **34**, 221 (1969).
[87] W. H. Haydl, Phys. Status Solidi **2**, K145 (1970).
[88] M. B. N. Butler and C. P. Sandbank, IEEE Trans. ED-**14**, 663 (1987).
[89] V. Mita, J. Appl. Phys. **42**, 2886 (1971).
[90] V. M. Rysakov, Pis'ma Zh. Tekh. Fiz. **16**, 68 (1990) [Sov. Tech. Phys. Lett. **16**, 510 (1990)].
[91] R. Katilyus, Fiz. Tverd. Tela **10**, 458 (1968) [Sov. Phys. Solid State **10**, 359 (1968)].
[92] Yu. V. Gulyaev, Fiz. Tekh. Poluprovodn. **2**, 628 (1968) [Sov. Phys. Semicond. **2**, 525 (1968)].
[93] T. E. Parker and R. Bray, Phys. Lett. **45A**, 347 (1973).
[94] J. Zucker and S. Zemon, J. Acoust. Soc. Am. **49**, 1037 (1970).
[95] A. M. D'yakonov, Yu. V. Ilisavskiĭ, and L. A. Kulakova, Fiz. Tverd. Tela **14**, 95 (1972) [Sov. Phys. Solid State **14**, 76 (1972)].
[96] Yu. V. Aristov and V. M. Rysakov, Pis'ma Zh. Tekh. Fiz. **15**, 47 (1989) [Sov. Tech. Phys. Lett. **15**, 19 (1989)].
[97] Yu. V. Aristov, L. N. Bolotov, and V. M. Rysakov, *ibid.* **14**, 924 (1988) [**14**, 409 (1988)].
[98] E. Mosekilde, Appl. Phys. Lett. **12**, 273 (1968).
[99] A. Ishida and Y. Inuishi, J. Phys. Soc. Jpn. **24**, 443 (1968).
[100] S. Furukawa, Jpn. J. Appl. Phys. **10**, 1642 (1971).
[101] V. V. Proklov, Yu. V. Gulyaev, and A. I. Morozov, Fiz. Tverd. Tela **14**, 968 (1972) [Sov. Phys. Solid State **14**, 832 (1972)].
[102] M. B. N. Butler, Rep. Prog. Phys. **37**, 431 (1974).
[103] V. L. Gurevich, R. Katilyus, and B. D. Laikhtman, Fiz. Tverd. Tela **10**, 2965 (1968) [Sov. Phys. Solid State **10**, 2347 (1969)].
[104] I. Bulberg and A. Many, Phys. Lett. A **24**, 705, 707 (1967).
[105] Yu. V. Gulyayev, E. F. Lushchenkova, and G. N. Shkerdin, Fiz. Tverd. Tela **22**, 150 (1980) [Sov. Phys. Solid State **22**, 85 (1980)].
[106] Yu. V. Gulyaev and G. N. Shkerdin, Zh. Eksp. Teor. Fiz. 77, 1396 (1979) [Sov. Phys. JETP **50**, 701 (1979)].
[107] Yu. Gulyaev, S. M. Movesesyan, and G. N. Shkerdin, Fiz. Tverd. Tela **22**, 523 (1980) [Sov. Phys. Solid State **22**,305 (1980)].
[108] V. M. Rysakov and Yu. V. Aristov, Fiz. Tverd. Tela **27**, 3413 (1985) [Sov. Phys. Solid State **27**, 2055 (1985)].
[109] V. M. Rysakov, Pis'ma Zh. Tekh. Fiz. **16**, 83 (1990) [Sov. Tekh. Fiz. Lett. **16**, 516 (1990)].
[110] D. V. Sitnikov and G. N. Shkerdin, Fiz.Tverd. Tela **29**, 1479 (1987) [Sov. Phys. Solid State **29**, 846 (1987)].
[111] R. Bercovicz and D. H. R. Price, Sol. State Comm. **14**, 195 (1974).
[112] L. E. Solov'ev, Vestnik LGU, No. 16, 170 (1967); No. 4, 23 (1968).
[113] V. B. Timofeev, Izv. AN SSSR **43**, 1233 (1979) [Bull. Acad. Sci. USSR, Phys. Ser. **43**(6), 120 (1979)].
[114] V. G. Lysenko, V. I. Revenko, T. G. Tramas, and V. B. Timofeev, Zh. Eksp. Teor. Fiz. **68**, 335 (1975) [Sov. Phys. JETP **41**, 163 (1975)].
[115] V. S. Dneprovskiĭ, V. I. Klimkov, and E. D. Martinenko, Fiz. Tverd. Tela **23**, 819 (1981) [Sov. Phys. Solid State **23**, 465 (1981)].
[116] V. M. Rysakov, L. L. Akatov, and Yu. V. Aristov, Pis'ma Zh. Tekh. Fiz. **9**, 621 (1983) [Sov. Tekh. Phys. Lett. **9**, 267 (1983)].
[117] A. A. Avetisyan, Yu. V. Gulyaev, and V. I. Mergorodskiĭ, *Propagation of Monochromatic Waves and Isolated Acoustic Signals Under Conditions of Acoustoelectronics Interaction* (Preprint of IRE AN SSSR No. 6 (424), M., 1985.

Translated by S. Chomet